

NOTICE WARNING CONCERNING COPYRIGHT RESTRICTIONS:

The copyright law of the United States (title 17, U.S. Code) governs the making of photocopies or other reproductions of copyrighted material. Any copying of this document without permission of its author may be prohibited by law.

Synthesis Of Evaporation Systems Using Minimum Utility Insights

by

J. B. Hillenbrand, Jr., A. W. Westerberg

EDRC-06-14-86-*

September 1986

**SYNTHESIS OF EVAPORATION SYSTEMS
USING MINIMUM UTILITY INSIGHTS**

by

John B. Hillenbrand, Jr.

and

Arthur W. Westerberg

**Department of Chemical Engineering
Carnegie-Mellon University
Pittsburgh, Pennsylvania 15213**

May 24, 1984

ABSTRACT

An evaporation system is a network of evaporators and heat exchangers which integrates an evaporation task with existing hot and cold process streams. This paper presents a systematic procedure for synthesizing evaporation systems which feature minimum utility use.

A first result in this paper shows that if a minimum utility $N+1$ -effect system does not contain the minimum utility N -effect system, it can be only marginally better. Given the feed and product temperatures, as well as the temperatures of the process streams, we use this insight to select the effect temperatures sequentially using a simple graphical procedure. A second set of results aids in the selection of the two most energy-efficient flowpatterns from among the $N!$ possible in an N -effect system. A third set of results shows where to introduce evaporator bypass. An algorithm is also presented which results in an evaporation system with equal effect areas.

We apply the proposed procedure to the design of a triple-effect evaporation system integrated with two process streams. The resulting minimum utility flowsheet requires 17 percent less steam than a more conventional triple-effect system design.

INTRODUCTION

Evaporation system synthesis is a relatively new area of process synthesis. Of the 190 articles published on process synthesis in the 1970's (Nishida *et al.* [14]), over one-fifth were concerned with heat exchanger network synthesis, while only one (Nishitani and Kunugita [15]) dealt with evaporation.

Most of the earlier evaporation publications (e.g. Standiford [21]) were written from a unit operations standpoint. Textbooks by Kern [7], McCabe and Smith [11], King [8], and the *Chemical Engineers' Handbook* [22] primarily address the analysis—not the synthesis—of evaporation systems.

Evaporator modeling has been the focus of several more recent publications (Harper and Tsao [3], Newell and Fisher [12], Holland [5], Stewart and Beveridge [23], Radovic *et al.* [18], and Newell [13]). However, all of these models were intended primarily for simulation, not synthesis.

Nishitani and Kunugita used an extension of the models by Harper and Tsao and by Holland to determine the optimal flowpattern of a multiple-effect system of up to twenty effects. One serious drawback of their approach is that the optimal flowpattern cannot be predicted *a priori*, requiring the simulation of all $N!$ flowpatterns for an N -effect system. In addition, they allow neither heat integration with process streams nor recovery of heat from condensate streams.

More recently, Nishitani and Kunugita [16] investigated a single-effect evaporator in conjunction with a jet condenser and heat exchanger, which allowed for preheating the feed with vapor from the evaporator. The operating conditions for the system were chosen based on a plot of annual investment cost versus annual exergy consumption. However, since the structure of their system was specified in advance, the paper primarily discussed the analysis—not the synthesis—of the evaporation system.

$$Q_{HU_0} \sim \left(V_T + \sum_{i=1}^N \frac{q_i}{\lambda_i} \right) \sum_{i=1}^N \Delta T_i$$

Equations (6) and (8) will be used extensively throughout the remainder of this paper. We shall refer to them as the *steam consumption equations*.

SELECTION OF EFFECT TEMPERATURES

This step is the first and most important of the synthesis technique because the effect temperatures play a major role in determining the energy-efficiency of the evaporation system. In fact, a utility target can be established based only on the number of effects and the effect temperatures. A graphical technique is used to select the effect temperatures which have the lowest utility target. This selection process is greatly simplified by a heuristic which is based on equation (8).

Equation (8) shows that the steam requirement of an evaporation system depends on four quantities: the total amount of vapor generated, V^{\wedge} the number of effects, N ; the heat of vaporization of each effect, X_i , $i = 1, N$; and the accumulated sensible heat for each effect, q_i , $i = 1, N$. V_y can be determined from the problem specifications, N is selected by the engineer, and the temperature dependence of X_i is known. However, the temperature dependence of q_i is not known. Fortunately, the construction of an appropriate "Problem Table" [9] will reveal the temperature dependence of q_i .

The example specifications given in Table 1 yield the Problem Table shown in Figure 3. The highest hot temperature (450 K) corresponds to the utility steam temperature while the lowest hot temperature (330 K) corresponds to the lowest allowable normal-boiling temperature of an effect. This temperature.

which is also the outlet temperature of the vapor condensate, is chosen based upon vacuum considerations. The remainder of the hot temperatures represent the feed stream ($T_c = 375$ K, $T_e + \Delta T^{HX} = 385$ K), product stream ($T_- = 415$ K, $T_- \cdot \Delta T^{\wedge} = 425$ K), inlet and outlet temperatures of all hot process streams (425 K, 360 K), and the inlet and outlet temperatures of all cold process streams plus ΔT^{HX} (350 K, 410 K). The cold temperatures are defined: $T_r = T_c - \Delta T^{HX}$. Note that the feed stream is divided into streams P and V, both entering at the feed temperature and proceeding directly to their respective outlet temperatures. The outlet temperature of V is shown as 335 K instead of 330 K because of the boiling point elevation. The vapor generated in any effect condenses at a temperature equal to the effect temperature minus the boiling point elevation, thus losing 5 K of temperature potential in this example.

The sensible heat requirement in each interval (q_{INT}) is calculated, with a positive value representing a heat deficit and a negative value representing a heat surplus. To obtain the accumulated sensible heat, q , for each interval, the heat loads in every interval are added from top to bottom. The profile of temperature versus q will be used to select the effect temperatures graphically. However, before illustrating the selection process, a required heuristic is first introduced.

Heuristic 1: The effect temperatures of the minimum utility N-effect system are contained in the minimum utility N+1-effect system.

Instead of simultaneously determining all the effect temperatures for a given evaporation system, this heuristic allows one to select the effect temperatures using a simple sequential procedure. For example, suppose that the effect temperatures have been determined for a double-effect system with minimum utility use. In synthesizing the minimum utility triple-effect system, only one new effect temperature must be chosen as the two from the double-effect

system are also included in the triple-effect flowsheet. We describe and justify this heuristic in Appendix B, where we show that, if the minimum utility N+1-effect system does not contain the minimum utility N-effect system, then it can only be marginally better than the N+1-effect system which does contain the optimal N-effect system.

Selection of the effect temperatures can be done graphically with the accumulated sensible heat curve we plot using the data calculated in Figure 3. After the effect temperatures are selected, they are included in an expanded form of the Problem Table, which we call an "Effect Temperature Diagram." As will be seen shortly, only the hot temperature scale of the Effect Temperature Diagram contains both the heat sources (hot utilities and condensing vapor streams) and the heat sinks (effect temperatures). Since the sensible heat requirements or surpluses must be calculated relative to both heat sources and sinks, T_{∞} is chosen as the ordinate for Figure 4, which shows the relationship between temperature and accumulated sensible heat. This q curve is a mirror image of both the "Heat Demand and Supply Curve" of Itoh *et al.* [6] and the "Grand Composite Curve" of Linnhoff *et al.* [10].

The steam consumption given by equation (8) is minimized by selecting effect temperatures with the smallest heats of vaporization *and* the smallest accumulated sensible heat requirements. For a single-effect system:

$$Q_{HU_0} \sim k \cdot \left(\frac{X}{T} \right) \quad (9)$$

or:

$$Q_{HU_0} \sim V X + q_1 \quad (10)$$

If one particular effect temperature has the smallest X and q , it should be selected. However, if such a temperature does not exist, then temperature selection is not as obvious. Consider selecting between two temperatures, T_1

and T_k , where we suppose that $T_j > T_k$, implying that $X_j < X_k$. In order for T_k to be considered further, q_k must be less than q_j . But how much less? If the amount of solvent to be vaporized in the effect is large, then q_k must be much less than q_j to compensate. If the amount of vapor generated is small, then the sensible heat terms have a greater impact on the steam consumption and a smaller difference between q_j and q_k could result in the selection of temperature T_k .

The selection of effect temperatures in a multiple-effect evaporation system can be formalized in the following way. Suppose that the N-effect evaporation system with minimum utility use (denoted by set S^A) has been found and that the temperature of effect N+1 is now sought. The two choices for the additional effect are temperatures T_j and T_k . Their respective steam consumption equations are:

$$Q_{HU_0}(S_{N^+} j) \sim [V_T \cdot (\sum_{i \in S_N} \xi_i) \cdot \Delta_j] (TTH)^2 (\Delta_j \cdot \sum_{i \in S_N} \lambda_i) \quad (11)$$

and:

$$Q_{HU_0}(S_{N^+} k) \sim [V_T + (\sum_{i \in S_N} \frac{\tilde{M}_i}{\lambda_i}) \cdot \frac{\tilde{M}_k}{\lambda_k} \cdot T_j] \cdot \Delta_k \cdot (\sum_{i \in S_N} \lambda_i)$$

If $Q_{HU_0}(S_{N^+} j) = Q_{HU_0}(S_{N^+} k)$, (11) and (12) can be combined and rearranged to form:

$$q_j \left(1 + \frac{1}{\lambda_j} \sum_{i \in S_N} \lambda_i \right) = q_k \left(1 + \frac{1}{\lambda_k} \sum_{i \in S_N} \lambda_i \right)$$

$$\sim \left(v_T + \sum_{i \in S_N} \frac{q_i}{\lambda_i} \right) (\lambda_k - \lambda_j) \quad (13)$$

The following approximation:

$$\left(1 + \frac{1}{\lambda_j} \sum_{i \in S_N} \lambda_i \right) \sim \left(1 + \frac{1}{\lambda_k} \sum_{i \in S_N} \lambda_i \right) \sim N + 1 \quad (14)$$

further simplifies equation (13):

$$q_j - q_k \sim \frac{1}{N + 1} \left(v_T + \sum_{i \in S_N} \frac{q_i}{\lambda_i} \right) (\lambda_k - \lambda_j) \quad (15)$$

If, in the accumulated sensible heat curve, a line is drawn through (q_j, T_j) and (q_k, T_k) , its slope would be:

$$\text{SLOPE}_{N+1} = \frac{T_j - T_k}{q_j - q_k} \sim (N + 1) \left(v_T + \sum_{i \in S_N} \frac{q_i}{\lambda_i} \right)^{-1} \left(\frac{T_j - T_k}{\lambda_k - \lambda_j} \right) \quad (16)$$

Since λ can be accurately approximated as a linear function of T , equation (16) reduces to:

$$\text{SLOPE}_{N+1} = \frac{T_j - T_k}{q_j - q_k} \sim - (N + 1) \left[\left(v_T + \sum_{i \in S_N} \frac{q_i}{\lambda_i} \right) \left(\frac{\partial \lambda}{\partial T} \right) \right]^{-1} \quad (17)$$

We shall use the slope expressed in (17) to select the effect temperatures. This slope increases as N increases because the amount of vapor generated in each additional effect decreases, making the sensible heat more important in the temperature selection process.

Selection of the effect temperatures begins with the calculation of the slope for the first effect. Note that set S_0 is empty.

$$\text{SLOPE}_1 = - (1) \left[(5 + 0) (-2.737) \right]^{-1} = 0.0731 \text{ K/kW} \quad (18)$$

A line with this slope is drawn in the upper left corner of Figure 5, where both q and λ are minimized, and moved downward and to the right until it intercepts a feasible effect temperature. In this example the steam temperature is 450 K. Since we require a ΔT_{\min} of 30 K for evaporators, the highest allowed actual temperature for effect 1 is $T_1 + \text{BPE} \leq 420$ K. The corresponding constraint on the normal-boiling temperature is $T_1 \leq 415$ K. The lowest allowed normal-boiling temperature of an effect is given as 330 K ($T_1 \geq 330$ K). The corresponding lowest allowed actual first effect temperature is $T_1 + \text{BPE} \geq 335$ K.

The two dashed lines with a slope of 0.0731 K/kW are shown for the first effect temperature selection. The upper line corresponds to $T_1 + \text{BPE}$, the actual effect temperature, while the line just below is $\text{BPE} = 5$ degrees lower and corresponds to the condensing temperature of the vapor raised in that effect. Ignoring the relatively small amount of heat available from the BPE degrees of superheat in steam raised in an effect before it starts to condense, we can argue that an evaporator can only supply heat to process streams which are colder than the condensing temperature of the steam it raises. It

can receive heat only from process streams hotter than $T_i + \text{BPE}$, the actual temperature of the effect. Thus if the process streams are acting as a heat source (positive slope) we use the q_i corresponding to the higher temperature, $T_i + \text{BPE}$. If the process streams are acting as a heat sink (negative slope), we select q_i corresponding to the lower temperature, T_i .

In Figure 5 the q curve has a positive slope in the region of the first effect. Thus, we choose $q^1 = -50 \text{ kW}$ at $T_j + \text{BPE} = 420 \text{ K}$, corresponding to the upper of the two dashed lines. Had the slope of the q curve been negative, we would have to select q_1 corresponding to the lower of the two dashed lines. In general we select the largest (rightmost) q_i intercepted by the two lines.

With the first effect operating at 420 K and having its vapor condense at 415 K, the highest actual effect temperature allowed for effect 2 is $AT_{\text{mm}}^{\text{EV}} = 30 \text{ mm}$ K below this condensing temperature, or 385 K. The corresponding highest normal-boiling temperature is $T_2 = 380 \text{ K}$. Referring to Figure 6, the second effect is chosen with a line of slope 0.147 K/kW:

$$\text{SLOPE}_2 = - (2) [(5 \cdot 10^{-5} \text{ W}) (1^{-2.737})]^{-1} \quad (19)$$

where:

$$330 \text{ K} \leq T_2 \leq 380 \text{ K}$$

Note that the slope has increased for the second effect, as discussed earlier. The temperature selected on Figure 6 for effect 2 is $T_2 = 330 \text{ K}$ and $q_2 = -665 \text{ kW}$. Finally the third effect temperature is chosen using the slope:

$$\text{SLOPE}_3 = - (3) [(5 \cdot 10^{-5} \text{ W}) (1^{-2.737})]^{-1} = 0.233 \text{ K/kW} \quad (20)$$

where:

$$365 \leq T_3 \leq 380 \text{ K}$$

T_3 is chosen to be 365 K on Figure 6.

Heuristic 1 allows the selection of the effect temperatures to be sequential instead of simultaneous. In the order of selection, the three effects are (q_i , T_i): (-50, 415); (-665, 330); and (-80, 365). These temperatures are added to the Problem Table in Figure 3 to produce an Effect Temperature Diagram (ETD). We shall construct two types of ETD's: preliminary and detailed. The Preliminary ETD, which is flowpattern-independent, is shown in Figure 7. The Detailed ETD, which includes the various evaporator streams flowing from effect to effect, will be described in a later section. In order to construct either diagram, the following temperatures must be added to the existing Problem Table for each effect i , $i = 1, N$:

- Hot temperatures: T_{ii} , $T_i + \text{BPE}$, $T_i + \text{BPE} + \text{AT}_{mm}^{H,X}$
- Cold temperatures: $T_i - \text{AT}_{mm}^{H,X}$, $T_i + \text{BPE} - \text{AT}_{mm}^{H,X}$, $T_i + \text{BPE}$

Temperature T_i must appear on the hot temperature scale because vapor from effect i condenses at this temperature and cools to temperature T_{LOW} acting as a heat source. The actual effect temperature $T_i + \text{BPE}$ must appear on both the hot and cold temperature scales because, depending on the flowpattern, the feed to any effect could be either hot or cold. All other temperatures listed above are either T_i or $T_i + \text{BPE}$ offset by $\text{AT}_{mm}^{H,X}$.

It has been shown that the accumulated sensible heat curve can help the engineer choose the potential effect temperatures as well as the order of selection. The q_i value for each effect temperature can be used to develop a rough utility target. The Preliminary ETD is constructed to estimate more accurate utility targets than those obtained graphically from the q curve. The Preliminary ETD is more accurate because it distinguishes between the two types of heat transfer, direct and indirect, whereas the q curve does not.

DIRECT AND INDIRECT HEAT TRANSFER

Direct heat transfer occurs when the feed to an effect is hotter than the effect itself. Suppose that the temperature of the feed stream is 375 K and the actual temperature of the effect is 370 K. The heat released by the stream in cooling from 375 K to 370 K can be added to the effect because the feed stream mixes directly with the boiling solution. Therefore, direct heat transfer, with an effective AT_{min} of zero, must be recorded separately from indirect heat transfer. The heat loads of all hot evaporator streams (in this case, V_T) within AT_{min}^{HX} of an effect temperature are recorded in the q_{DIP}^{Δ} column of Figure 7.

The heat loads of all remaining streams (process streams, cold evaporator streams, and the indirect portions of the hot evaporator streams) are recorded in the q_{MU} column. These indirect heat loads have a AT_{min}^{HX} of 10 K with respect to the effect temperatures. The direct and indirect heat loads are merged to the appropriate temperature levels and are recorded in the third column. q_{MERG}

Referring to Figure 7, the first non-zero heat load of -50 kW is shown in the interval between 425 K and 420 K on the hot temperature scale. This value is simply the heat required by cold stream P minus the heat available from hot stream H1. The negative sign indicates that an excess of 50 kW exists in that interval, **or that 50 kW** of heat are available at 420 K. Because this heat excess is not AT_{min}^{**} hotter than effect 1, it cannot supply heat to that effect, which operates at 420 K. Therefore, the -50 kW are cascaded to a lower temperature level and the value of $q_{K,CD} \sim_c$ for this interval is zero.

A similar argument takes place in the interval between 420 K and 415 K, which has a q_{IND} of -50 kW and a Q_{MERGC} of 0. However, in the interval between 415 K and 410 K, the -50 kW heat load is below T_1 (415 K) and well

above T_2 * BPE (370 K). Therefore, this heat excess can be applied to effect 2. The value of $q_{McRGc}^{JCO_C}$ for this interval is -50 kW plus the two -50 kW heat loads cascaded from above.

The indirect heat load becomes positive in the interval between 410 K and 385 K because cold streams P and C₁-require more heat than is available from hot stream H₁.

Continuing down the diagram, the indirect heat requirement between 385 K and 380 K is -25 kW. Since this heat source is at least AT_{mm}^{HX} above effect 2 (370 K), it can be applied to the effect. Because of this, the indirect heat load of -25 kW appears in the Q_{MERGE} column.

An indirect heat load of -25 kW also exists in the interval between 380 and 375 K. In this instance, however, this heat excess is not AT_{mm}^{MX} hotter than effect 2. Therefore, it cannot supply heat to the effect and must be cascaded to the next available level. The value of Q^{pQg} in this interval is zero.

The same situation arises in the interval between 375 and 370 K. The 25 kW indirect heat excess, which cannot be applied to effect 2, is cascaded down to the next available level. The direct heat load of -105 kW, however, can be applied to effect 2. As a result, $q_{McRGc}^{JCO_C}$ equals q_{DIR}^{\wedge} in this interval.

The interval from 370 K (actual temperature of effect 2) to 365 K (normal-boiling temperature of effect 2) has an indirect heat excess of 130 kW. If this heat load had been positive, it would be included in Q_{MERGE} because a heat requirement reduces the amount of heat available to an effect. However, since this heat load is negative, it too is cascaded to the next available level.

Finally, another indirect load of -130 kW is shown between 365 K and 360 K. Since this heat excess is below the normal-boiling temperature of effect 2

and well above effect 3, it is not cascaded to a lower level. The value of q_{-CDrc} for this interval is -310 kW. This is merely the indirect heat load in this interval (-130 kW) plus all indirect heat loads cascaded from higher levels (-25, -25, and -130 kW).

If all indirect heat loads are positive, then for any interval Q_{MERGE}^{15} simply q_{QIR} plus q_{IND} . However, when q_{JND} is negative, the value of Q_{MERGE} depends on the location of this indirect heat excess relative to the effect temperatures.

The values of Q_{MERGE}^m the remaining intervals were determined in a similar manner. Finally, the improved estimates of q_i were obtained by adding the Q_{MERGE} values from top to bottom. The three potential effect temperatures, heats of vaporization, initial estimates of q_i , and improved estimates of q_i are given in Table 2. Using equation (6), the preliminary utility targets, $CL_{HU_0}^i(T_i; i = 1, N)$, are calculated for systems of one through three effects.

One effect:

- $Q_{HU_0}^{(415)} = 10670 \text{ kW}$
- $Q_{HU_0}^{(330)} = 11170 \text{ kW}$
- $Q_{HU_0}^{(365)} = 11320 \text{ kW}$

Two effects:

- $Q_{MU_0}^{(415, 330)} = 5296 \text{ kW}$
- $Q_{HU_0}^{(415, 365)} = 5486 \text{ kW}$
- $Q_{WU_0}^{(365, 330)} = 5454 \text{ kW}$

Three effects:

- $Q_{HU_0}^{(415, 365, 330)} = 3534 \text{ kW}$

The above utility targets aid in the selection of both the number of effects and the effect temperatures. In this paper, the triple-effect system is chosen

to illustrate the remaining steps in the synthesis technique. Now that the number of effects and the effect temperatures have been chosen, the issues of flowpattern and bypass are addressed.

SELECTION OF EVAPORATOR FLOWPATTERN AND BYPASS

The selection of flowpattern, the path the liquid takes in the evaporation system, is now addressed. For an N -effect system, there are $N!$ basic flowpatterns from which to choose. For example, there are 720 possible flowpatterns for a six-effect system. Figure 8 shows the six basic flowpatterns for a triple-effect system. In general, the effects are numbered 1 through N , with 1 the hottest and N the coldest. Referring to Figure 8 and going from top to bottom, the flowpatterns are 123, 132, 213, 231, 312, and 321. Flowpatterns 123 and 321 are also called forward feed and backward feed, respectively, while the other flowpatterns are called mixed feed.

The following is the simplest and most common flowpattern heuristic [19] :

- High feed temperature \Rightarrow forward feed
- Low feed temperature \Rightarrow backward feed
- Intermediate feed temperature \Rightarrow mixed feed

This heuristic, while it does identify a general flowpattern trend, does not help in selecting from among the $N! - 2$ mixed flowpatterns.

The utility use of any particular flowpattern can be determined by constructing a Detailed Effect Temperature Diagram, which has the same temperature intervals as the Preliminary ETD. The utility target established by the Preliminary ETD can be approached by the correct selection of the flowpattern.

Recall that the product and vapor streams in the Preliminary ETD proceed directly from the feed temperature to their respective outlet temperatures. The

flowpattern with minimum utility use will have evaporator streams which most closely resemble this behavior. In many cases, however, the effect temperatures are chosen outside of the range between the feed and product temperatures. This means that the evaporator streams must make a "U-turn" somewhere in the system, i.e. the feed to an effect is a cold stream while the product from that effect is a hot stream, and vice versa.

The flowpattern which approaches the the utility target of the Preliminary ETD should have as few U-turns as possible. The minimum number of U-turns ranges from zero (when all effect temperatures are placed between the feed and product temperatures) to two (when both the hottest and coldest effects are placed outside this range).

Our work has shown that, in principle, one should need to consider at most two methods of feeding: feed temperature to hottest effect to coldest effect to product temperature or feed temperature to coldest effect to hottest effect to product temperature. The question is whether the feed stream should enter the intermediate effects on the way up or on the way down.

A simple heuristic which is valid for virtually all evaporation systems without bypass has been developed. This heuristic, which is defined below, is described and justified in Appendix C.

Heuristic 2: An evaporation system feed stream, in following the most direct path from feed temperature to product temperature without bypass, should enter any effect that does not already have a feed stream. This can be restated: an evaporator feed stream should not skip an effect that it is approaching for the first time.

As mentioned above, one of the two potential methods of feeding is: feed temperature to hottest effect to coldest effect to product temperature.

Returning to our example, both the feed and product temperatures lie between effects 1 and 2. Because of the feed location, the flowpattern should begin with effect 1. In going from effect 1 to effect 3 to the product temperature, flowpatterns 123 and 132 are possible. According to Heuristic 2, the product from effect 1 should not skip effect 2, making the preferred flowpattern 123.

A similar argument takes place for the alternate method of feeding: feed temperature to coldest effect to hottest effect to product temperature. Since the product temperature lies between effects 1 and 2, the flowpattern should end with effect 1. The path from feed temperature to coldest effect to hottest effect can be described by either 231 or 321. But since effect 2 lies between the feed temperature and effect 3, it should not be skipped. Therefore, the best flowpattern for this method of feeding is 231.

Instead of six flowpatterns to consider, only two remain: 123 and 231. A final rule of flowpattern screening can be illustrated with Figure 9: the hot and cold evaporator streams should overlap as little as possible. In Figure 9 two methods of feeding are shown for a system with hot feed and cold product. The pattern shown on the left, feed temperature to hottest effect to coldest effect to product temperature, features much less overlap than the one on the right, feed temperature to coldest effect to hottest effect to product temperature. This overlap will manifest itself in heat exchanger area because as the amount of overlap increases, the more heat is transferred from hot streams to cold streams.

Figure 10 shows the flowpatterns 123 and 231. From the overlap rule, it appears that 231 is slightly better than 123. This is reflected in Table 3, which shows the steam consumption for all six possible flowpatterns. The steam consumption for each flowpattern was calculated by constructing a Detailed Effect Temperature Diagram, which will be discussed shortly.

EVAPORATOR BYPASS

At this point in the synthesis procedure, the following design decisions have been made: number of effects ^s 3; actual effect temperatures = 420, 370, and 335 K; and the two potential flowpatterns are 123 and 231. Evaporator bypass, which has been ignored to this point, can now be addressed. Evaporator bypass is simply a portion of an evaporator feed stream which does not enter an effect. Although it is not always beneficial, bypass can reduce the utility requirement as well as the capital cost of many evaporation systems.

Heat transfer in evaporation systems occurs in both evaporators and heat exchangers. Shown in Table 4 is a comparison of the incremental cost per unit area of both evaporators and heat exchangers. The cost data is based on the work of Guthrie [2]. For a given area, the incremental cost of evaporators is approximately two to six times the cost of heat exchangers. It is obvious that in most situations, even in the case of a large evaporator versus a small heat exchanger, additional heat exchanger area is less expensive than additional evaporator area.

If the feed to an evaporator is colder than the effect, bypassing a portion of the feed can reduce the amount of heat transfer occurring in that effect at the expense of additional heat exchanger area. In addition, a reduction in steam use may result from this bypass. On the other hand, bypassing a **portion of a hot feed stream** reduces the amount of direct heat available, which increases both the utility bill and the capital cost.

Figure 11 shows how the bypass stream affects the sensible heat requirement of an effect at temperature T . The effect temperature is higher than feed temperature T_F , which is higher than product temperature T_P . In this simple analysis, boiling point elevation is neglected. This assumption, however, does not affect the results of this analysis in any way. Feed stream

F splits into bypass stream B and evaporator feed stream F-B. Vapor stream V and evaporator product stream F-B-V both cool to temperature T_p , while bypass stream B proceeds directly from feed temperature T_p to product temperature T_p . The sensible heat requirement of the effect is determined by adding all heat loads from the heat source to temperature T (on the hot scale). This heat requirement is $(F_{C_r} - F_{C_Q})AT_{HX}$. If the flowrate of the bypass stream is maximized, the heat requirement is minimized. In this case, evaporator bypass reduces both the utility use and the capital cost because the smaller sensible heat requirement results in a smaller evaporator area.

In a similar manner, all other possible configurations were investigated by permutating hot temperatures $T^*AT_{HX}^{\min}$, T_p , $T_p + AT_{HX}^{\min}$, T_c , $T_c + AT_{HX}^{\min}$, and T_D (thirty cases in all). Evaporator bypass was found to be desirable when:

- $T \leq T_c \leq T^p$ (reduces utility use and evaporator area)
- $T \leq T_p \leq T_c$ (reduces utility use and evaporator area)
- $T_p \leq T \leq T^p$ (reduces evaporator area only)

On the other hand, bypass is not desirable when:

- $T_p \leq T \leq T_p$ (increases utility use and evaporator area)
- $T_p \leq T_p \leq T$ (increases utility use and evaporator area)
- $T_p \leq T_p \leq T$ (increases evaporator area only)

These rules can be simplified:

- If $T_c \leq T$, do not bypass the effect
- If $T_c \leq T$, bypass the maximum amount

Recent work has shown that bypass can give rise to flowpatterns which differ from those predicted by Heuristic 2. When bypass is allowed, the flowpattern should be selected with the following rule:

Heuristic 3: An evaporation system feed stream, in following the most

direct path from feed temperature to product temperature, should skip an effect only if the feed is cold. A hot evaporation system feed stream should enter any effect that does not already have a feed stream. In addition, there should be no bypass of this effect. A cold feed stream, however, should skip an effect that it is approaching for the first time. The feed entering this effect should be minimized, thus maximizing the bypass stream.

Heuristic 3 has not been demonstrated in general, but has been verified numerically with other example problems. The authors are working on arguments similar to those in Appendix C to quantify the benefits of skipping an effect with cold feed.

The flowpattern and bypass streams can be selected by following the feed stream through the evaporation system for each method of feeding. For the example problem in this paper, flowpatterns 123 and 231 are again chosen for the two respective methods of feeding. Based on the feed, product, and effect temperatures, the opportunity for cold feed to skip effect 2 never presents itself. Therefore, the flowpatterns chosen by Heuristic 2 are the same as the flowpatterns chosen when bypass is allowed. For flowpattern 123, the feed stream (375 K) is colder than effect 1 (420 K). This gives rise to a bypass of effect 1. Effect 1 is hotter than effect 2 and effect 2 is hotter than effect 3. Therefore, there should be no bypass of effects 2 and 3. Similarly for flowpattern 231, the feed is hotter than effect 2 (370 K), which in turn is hotter than effect 3. Effect 3, however, is colder than effect 1, indicating that bypass of effect 1 is desirable. Now that the bypass streams have been chosen, the utility requirements of the two respective flowsheets can be calculated in attempt to find the minimum utility flowsheet.

DETERMINATION OF UTILITY USE AND SYSTEM FLOWRATES

The actual utility use can be determined by constructing a Detailed Effect Temperature Diagram. Shown in Figure 12 is the Detailed ETD for flowpattern 123 with bypass. The temperature intervals are identical to those in the Preliminary ETD, but all evaporator streams are now shown as they will appear in the system[^] flowsheet.

Feed stream F originates at 375 K. Bypass stream B does not enter effect 1, but flows directly into effect 2 at 370 K. The remainder of the feed stream (F - B) is the feed to effect 1 at 420 K. The vapor generated in effect 1 condenses at 415 K and cools to 330 K. The product from effect 1 (F - B - V[^]) combines with bypass stream B to become the feed to effect 2 at 370 K. Vapor stream V₂ condenses at 365 K and cools to 330 K. The product from effect 2 (F - V₁ - V₂) feeds directly into effect 3, generating vapor stream V₃ (not shown) and product stream P. Stream P is heated from 335 K to the desired product temperature, 415 K. In addition to the evaporator streams, process streams H1 and C1 appear as they do in the Preliminary ETD.

The heat loads are then determined for each temperature interval. The portions of the feed streams to effects 2 and 3 which are within $\Delta T_{\text{HX}}^{\text{mm}}$ of the effect temperatures are recorded in the direct heat transfer column. The heat loads for all remaining streams are listed in the indirect heat transfer column. The heat loads are then combined and recorded in the q_{-CDr-c} column. The q_{MERGE} values are then added from top to bottom to obtain q₁.

The steam consumption is calculated using equation (6):

$$Q_{\text{H}_2\text{O}} = \left(V_T + \sum_{i=1}^N \frac{q_i}{\lambda_i} \right) \left(\sum_{i=1}^N \frac{1}{\lambda_i} \right)^{-1} \quad (6)$$

where:

$$q_1 = 310 - 10FC_B \text{ kW}$$

$$q_2 = 70 + 5FC_{V_1} \text{ kW}$$

$$q_3 = -665 + 15(FC_{V_1} + FC_{V_2}) \text{ kW}$$

$$\lambda_1 = 2134, \lambda_2 = 2271, \lambda_3 = 2367 \text{ kJ/kg}$$

Initial guesses of FC_{V_1} , FC_{V_2} , and FC_B were based on the assumption of equal vaporization in each effect. Q_{HU_0} was then calculated, with the following modification of equation (4) used to update FC_{V_1} :

$$V_1 = \frac{Q_1}{\lambda_1} = \frac{Q_{HU_0} - q_1}{\lambda_1} \quad (21)$$

or:

$$FC_{V_1} = \left(\frac{Q_{HU_0} - q_1}{\lambda_1} \right) C_{P_0} \quad (22)$$

FC_{V_2} is updated in a similar manner:

$$FC_{V_2} = \left(\frac{Q_{HU_0} - q_2}{\lambda_2} \right) C_{P_0} \quad (23)$$

The bypass stream updates are based on Figure 13. Evaporation system feed stream F is split into a bypass stream (flowrate = B , concentration = X_F) and the feed to effect 1 (flowrate = $F - B$, concentration = X_F). In order to maximize the bypass stream, thus minimizing the utility requirement, the product stream from effect 1 (flowrate = $F - B - V_1$, concentration = X_1) must have a concentration of X_{\max} , the maximum allowable solute concentration:

$$X_1 = \frac{(F - B)X_F}{F - B - V_1} = X_{\max} \quad (24)$$

This equation can be rearranged to solve for B and FC_B :

$$B \cdot F = (\bar{X}_m^A) \quad (25)$$

$$\max F \quad (26)$$

Beginning with starting guesses based on equal vaporization in each effect and using (22), (23), and (26) to update these guesses, equation (6) converged in only three iterations. The converged values obtained were $Q_{MU_0} = 3663$ kW, $FC_1 = 7.107$ kW/K, $FC_2 = 6.578$ kW/K, and $FC_3 = 25.848$ kW/K. With these values known, all remaining flows were obtained by simple material balances.

The utility use of flowpattern 231 with bypass was calculated in a similar manner. Cl_{HU_0} for this system was found to be 3692 kW, one percent higher than flowpattern 123. This difference in steam consumption arose from the difference in the bypass streams.

Recall that in both flowpattern 123 and 231, effect 1 was bypassed as much as possible. In flowpattern 123, the concentration of the feed to effect 1 was 0.20, while in flowpattern 231, this concentration was approximately 0.30. As a result, it was possible to have a larger bypass stream for flowpattern 123 than for 231. Thus, flowpattern 123 with bypass of effect 1 is the minimum utility flowsheet, albeit only marginally so.

Now that the number of effects, effect temperatures, evaporator flowpattern, bypass, and all stream flowrates have been specified, the only task remaining is to generate the final flowsheet.

DETERMINATION OF THE FLOWSHEET STRUCTURE

This final step of the synthesis procedure is very similar to the final step of heat exchanger network synthesis. However, the two procedures differ somewhat because of the presence of direct heat transfer.

Neither a T-Q diagram nor a "Grand Composite Curve" of the entire evaporation system provides much insight at this point because direct heat transfer indicates an apparent AT which is less than AT_{mm}^{HX} . The cost differential between evaporators and heat exchangers motivates the engineer to design a heat recovery network with minimum evaporator area and maximum heat exchanger area. However, minimizing the evaporator area may cause the flowsheet to have several very small heat exchangers. Instead of requiring minimum evaporator area, a more practical goal is to seek the flowsheet with the minimum number of heat exchangers.

The presence of both direct and indirect heat transfer further complicates matters. Fortunately, a heat exchanger network can be obtained by using the method of either Cerda *et al.* [1] or Papoulias and Grossmann [17].

In both publications, linear programming formulations were used to model heat exchanger networks. Cerda *et al.* used a linear program formulation known as the "Transportation Problem", while Papoulias and Grossmann used the "Transshipment Model" as the basis for their method. The basic idea of both formulations is to treat heat as a commodity which is shipped from origins (hot streams) to destinations (cold streams). These heat shipments are subject to thermodynamic constraints (enforcement of AT_{min}^{\wedge} in all heat exchanger matches). Based on the objective function, one can obtain the heat exchanger network with minimum utility use, minimum number of heat exchangers, or some combination of the two. But the real advantage of these formulations is that heat exchanger networks with restricted matches or preferred matches can be synthesized.

An evaporation system with all streams specified can also be thought of as a restricted match heat exchanger problem. For example, a hot evaporator feed stream within AT_{mm}^{HX} of an effect can supply heat to the effect, while a

hot process stream in that same interval cannot. Moreover, since evaporators are more costly than heat exchangers, heat transfer occurring in heat exchangers is preferred over heat transfer in evaporators. The cost coefficient for each hot stream/cold stream match is chosen based on the feasibility of the match and whether the transfer of heat takes place in evaporators or heat exchangers.

Referring to the example problem, the heat capacity flowrates, inlet temperatures, and outlet temperatures of all 9 streams shown in the Detailed ETD are now known. Even so, integrating this number of streams in a network of 3 evaporators and several heat exchangers is not a trivial problem. Fortunately, one characteristic of evaporation systems--multiple pinch points--can be exploited to reduce the size of the problem. In general, an N-effect evaporation system has N pinch points. The region between each pinch point can be treated as an independent subproblem, making generation of the heat recovery network a much simpler task.

In Figure 12, the first partition is drawn at $T_H = T_1 = 415$ K. Partition 1 is composed of the first four temperature intervals and contains only 4 streams: H1, P₁, F₁, and P. Shown in Figure 14 is the tableau for partition 1. The four temperature intervals are numbered from 1 to 4. For example, H1,3 denotes the heat given up by stream H1 in cooling from 425 K to 420 K. Likewise, F₁,3 represents the heat required by stream F₁ in heating from 410 K to 415 K. A total of three hot streams (Q_{HU_0} ; H1,3; and H1,4) and six cold streams (Q_{V_1} ; F₁,2; F₁,3; F₁,4; P,3; and P,4) are shown in Figure 14. Note that even though stream P₁ appears in temperature interval 4 in Figure 12, it is not included in the tableau. The indirect heat load in temperature interval 4 is given as $-50 + 5FC_{V_1} = -15$ kW. This heat load (remember, negative load means heat is available) cannot be applied to effect 1 because it is below the temperature at which effect 1 operates. It is cascaded to the next interval. Therefore, either

H1#4 or P₁.4 must be reduced by 15 kW. By coincidence, P₁ gives up 15 kW in cooling from 420 K to 415 K. Thus, stream P_{1#4} appears in partition 2, not partition 1.

Figure 14 indicates that all the steam required by the system is used in effect 1. Since 53 kW of steam η are used to satisfy the sensible heat requirement of stream F₁, we can calculate the temperature of the feed entering effect 1. We also see that stream H1 must supply the remainder of the heat required by F₁ and all of the heat required by stream P.

Partitions are also drawn at $T_H = T_2 = 365$ K and $T_3 = 330$ K. The resulting tableaux can usually be solved by hand because of their relatively small size. Larger tableaux could be solved with linear programming software such as LINDO (Schrage [19]).

The heat exchanger network for each partition is merged to obtain the total system flowsheet, as shown in Figure 15. This flowsheet features minimum utility use, minimum number of heat exchangers, and minimum evaporator area, in that order. In other words, the strategy in this portion of the procedure is first to determine the minimum utility use and all system flows. Then, using a Transportation Problem tableau, determine the minimum number of heat exchangers. Finally, with a finite number of heat exchangers given, minimize all evaporator areas.

At this point the engineer has the option of modifying the flowsheet in order to reduce further the number of heat exchangers, eliminate stream splitting, etc. These alterations, which increase the utility use, can be accomplished in two ways. The simplest way is to shift positive heat loads (heat requirements) upward in the Detailed ETD. This results in a "less pinched" heat recovery network, making selection of the heat exchanger

matches easier and possibly reducing the number of heat exchangers required. The second way of altering the flowsheet is to choose heat exchange matches between two or more streams in advance. Then include only the unmatched portions of those streams in the Detailed ETD. It must be stressed that either of these modifications will increase the utility use and will also require the construction of a new Detailed ETD. However, if the heat recovery network has restricted matches or other complications, the above procedures are necessary to ensure both minimum utility use and feasibility, subject to these restrictions.

If the structure of the flowsheet is satisfactory, the synthesis procedure is complete. A cost estimate for this flowsheet should now be performed.

From a capital cost standpoint, it is often desirable for all effects to have the same area. Effects with equal areas are less expensive to fabricate and easier to maintain than effects with unequal areas. However, the synthesis method presented to this point does not guarantee equal areas. In fact, the flowsheet in Figure 15 has effect areas of 57.1, 42.5, and 80.3 m². Fortunately, fully integrated evaporation systems with equal effect areas can be obtained to compare with the above results using the algorithm presented in the following section.

ENFORCEMENT OF EQUAL EFFECT AREAS

Energy-efficient evaporation systems can also be obtained without requiring unequal effect areas and exotic bypass schemes. In this section, a triple-effect system with no bypass and equal effect areas is synthesized. The resulting flowsheet represents a modest but still significant improvement in terms of estimated annual cost, compared with the best flowsheet obtained using the model of Nishitani and Kunugita [15].

The procedure to obtain equal effect areas is:

1. For a given number of effects and an assumed value of AT^{EV} , use the graphical synthesis procedure to choose the minimum utility effect temperatures.
2. Based on the feed, product, and effect temperatures, determine the flow pattern and bypass scheme.
3. Construct a Detailed Effect Temperature Diagram to obtain all stream flows.
4. Use the above result and divide the problem into N partitions to determine the heat recovery network.
5. Solve the problem twice: first to find the minimum area for each effect and then to find the maximum area for each effect. In both solutions, minimum utility use still results.
6. Partition the effects into alternative combinations of those sharing common area ranges. For example, in a triple-effect system, effects 1 and 2 may share overlapping area ranges and effects 1 and 3 also, but not 2 and 3. In this case one could select the two evaporators having the smallest area in common with effects 1 and 2 or with effects 2 and 3, and then purchase the remaining effect separately. At this point one sees a natural partitioning which can maintain minimum utility use. If it is desired that more or all effects have overlapping areas and as yet do not, then continue to step 7.
7. If the areas do not overlap as desired, choose new effect temperatures and go to step 2.

When this procedure is complete and the evaporator areas are known, the heat exchanger network can then be determined easily. The goal is then to minimize the number of heat exchangers.

Returning to the example problem. Table 3 showed that the minimum utility flow pattern without bypass was 231. After constructing a Detailed Effect Temperature Diagram and solving for all stream flow rates, the problem was divided into three partitions. Each partition was solved twice to obtain bounds on the area of each effect. The area of effect 1 was found to be 57.7 m^2 . Effect 2 ranged from 43.5 to 44.2 m^2 , while effect 3 varied from 75.9 to 83.5 m^2 . The following equation was used to alter the effect temperatures:

$$\left(\Delta T_i^{EV}\right)_{\text{new}} = \left(\frac{A_i}{A_{\text{mean}}}\right)\left(\Delta T_i^{EV}\right)_{\text{old}} \quad i = N, N-1, \dots, 2 \quad (27)$$

The temperature of effect N is held constant while the remaining effect temperatures are varied. In this way, the available temperature range is kept as large as possible, enhancing the probability of attaining equal areas. Shown in Table 5 is a summary of the temperature selection and the resulting effect areas. Note that in the second iteration, the minimum utility flowpattern became 321 when the temperature of effect 2 moved above the feed temperature. Equal effect areas were obtained in only three iterations, yielding the flowsheet shown in Figure 16.

The model of Nishitani and Kunugita was used to produce the flowsheet in Figure 17. Note that the process streams are not integrated into the evaporation task. As a result, the steam requirement of this flowsheet is 17 percent greater than the flowsheet in Figure 16 and 20 percent greater than the minimum utility flowsheet in Figure 15. Shown in Table 6 is a comparison of the annual utility and capital costs of the three flowsheets. Even though the integrated flowsheets have higher capital costs than the non-integrated one, the savings in steam and cooling water more than compensate. If the utility costs were higher or if a payback period greater than 2.5 years were used, the integrated flowsheets would be even more attractive.

Another example problem with 4 effects, equal effect areas, and no process streams has been examined. In this case, our minimum utility flowsheet required 44 percent less steam than the best non-integrated flowsheet. In addition, the capital costs of the two flowsheets differed by less than 1 percent. Obviously, significant energy savings are possible with this synthesis technique, with or without process streams.

CONCLUSIONS

The purpose of this paper was to demonstrate that it is possible to synthesize evaporation systems which feature minimum utility use. Moreover, these highly integrated flowsheets require much less energy than conventional non-integrated systems. Our synthesis procedure can be summarized:

1. Select the number of effects and effect temperatures based on a preliminary utility target.
 - a. Construct an appropriate Problem Table (Figure 3).
 - b. Construct an Accumulated Sensible Heat (q) Curve (Figure 4) based on the Problem Table.
 - c. Select the potential effect temperatures by passing lines of increasing slope (Equation 16) through the q curve (Figures 5 and 6).
 - d. Construct a Preliminary Effect Temperature Diagram (Figure 7) to establish a lower bound on the utility use as a function of the number of effects and the effect temperatures (Equation 6).
2. Select the evaporator flowpattern and bypass with the following two simple rules:
 - a. If bypass is not allowed, use Heuristic 2: An evaporation system feed stream, in following the most direct path from feed temperature to product temperature without bypass, should enter any effect that does not already have a feed stream. This can be restated: an evaporator feed stream should not skip an effect that it is approaching for the first time.
 - b. If bypass is allowed, use Heuristic 3: The evaporation system feed stream should again follow the most direct path from feed temperature to product temperature. A hot evaporation system feed stream should enter any effect that does not already have a feed stream. In addition, there should be no bypass of this effect. A cold feed stream, however, should skip an effect that it is approaching for the first time. The feed entering this effect should be minimized, thus maximizing the bypass stream.
3. Set all flows in the system and determine the actual utility use (Equation 6) by constructing a Detailed Effect Temperature Diagram (Figure 12).
4. Divide the problem into partitions (Figure 14) to obtain the heat recovery network. If the flowsheet (Figure 15) is satisfactory, stop.

5. If equal effect areas are required, solve each partition twice to obtain upper and lower bounds on the area of each effect. If the areas overlap, draw the flowsheet (Figure 16). Otherwise, alter the effect temperatures (Equation 27) and go to step 2.

Step 1 of the algorithm requires the assumptions of negligible heat of mixing and constant boiling point elevation. If these assumptions are not valid for the system under investigation, the predicted utility target will not be as accurate as it would be for a more ideal system. For most systems, this method of effect temperature selection is still more sensible than simply dividing the temperature scale into equal AT segments.

The Detailed Effect Temperature Diagram can accommodate heat of mixing, variable boiling point elevation, heat loss terms, and other non-idealities. The authors have used the above procedure to synthesize a triple-effect NaOH/water evaporation system with equal effect areas. For this problem, heat of mixing was significant while the boiling point elevation ranged from 13 K to 39 K.

The synthesis technique also has application to retrofit design tasks. If the number of effects and effect temperatures are already specified, a Detailed ETD can provide the engineer with a useful minimum utility target. A Detailed ETD can also reveal the increase in utility use if certain heat exchanger matches are chosen.

This work has shown that significant utility savings can result from the integration of process streams with evaporation streams. As the number of effects increases, the potential energy savings also increase. This reduction in utility use is usually accomplished with little or no additional capital cost. For an evaporation system of 4 effects, we have calculated energy savings of over 40 percent.

NOMENCLATURE

A_i	Area of effect i (m^2)
A_{mean}	Average area of all N effects (m^2)
B	Flowrate of evaporator bypass stream (kg/s)
BPE_i	Boiling point elevation in effect i (K)
ETD	Effect Temperature Diagram
F	Flowrate of feed to evaporation system (kg/s)
F_i	Flowrate of feed to effect i (kg/s)
FC_i	Heat capacity flowrate of stream i (kW/K)
$h_{C_{i-1}}$	Enthalpy of condensed vapor stream V_{i-1} at temperature T_{i-1} and at the pressure of effect $i-1$ (kJ/kg)
h_{F_i}	Enthalpy of stream F_i evaluated at temperature $T_i + BPE_i$ and concentration X_{F_i} (kJ/kg)
h_{P_i}	Enthalpy of stream P_i evaluated at temperature $T_i + BPE_i$ and concentration X_{P_i} (kJ/kg)
H_{V_i}	Enthalpy of stream V_i evaluated at temperature $T_i + BPE_i$ and at the pressure of effect i (kJ/kg)
h_{V_i}	Liquid enthalpy of stream V_i evaluated at temperature $T_i + BPE_i$ and at the pressure of effect i (kJ/kg)
N	Number of evaporator effects
P	Flowrate of product stream from evaporation system (kg/s)
P_i	Flowrate of product stream leaving effect i (kg/s)
q	Accumulated sensible heat requirement (kW)
$q_{C_{i-1}}$	Net amount of sensible heat required by cold streams at level $i-1$ (kW)
q_{DIR}	Heat available from hot evaporator feed streams (kW)
q_{H_i}	Net amount of sensible heat available from hot streams at level i (kW)
$Q_{HU_{i-1}}$	Amount of hot utility from level $i-1$ which is required by the evaporation system (kW)

Q_i	Heat available for vaporization in effect i (kW)
q_i	Accumulated sensible heat at level i (kW)
Q_{i-n}	Latent heat transferred from effect $i-1$ to effect i (kW)
Q, K, O $^{\wedge}IND$	Heat which is transferred based on AT_{mm}^{HX} (kW)
q_{INT}	Sensible heat requirement in any interval of the Problem Table (kW)
q_{MERGE}	Sensible heat requirement in any interval of an Effect Temperature Diagram after combining the direct and indirect contributions (kW)
S_N	Set of N effect temperatures with minimum utility use
$SLOPE_{N+1}$	Slope of line used to select effect temperature $N+1$ (K/kW)
T^F	Temperature of feed to evaporation system (K)
T_i	Normal-boiling temperature of effect i (K)
T_{lo}^w	Minimum allowable normal-boiling temperature of an effect (K)
T_p	Desired temperature of evaporation system product (K)
V_i	Flowrate of vapor leaving effect i (kg/s)
V_T	Total amount of vapor generated in evaporation system (kg/s)
X_p	Solute concentration of evaporator feed stream (kg/kg)
X_i	Solute concentration of product from effect i (kg/kg)
X_{max}	Maximum allowable solute concentration (kg/kg)
X_p	Solute concentration of evaporator product stream (kg/kg)
Greek letters:	
Δq_i	Difference in the sensible heat requirement of effect i for two different flowpatterns (kW)
ΔT_i^{\wedge}	Temperature difference between condensing vapor from effect $i-1$ and the actual temperature of effect i (K)
AT_{min}^{EV}	Minimum allowable temperature drop from effect to effect (K)
AT_{min}^{HX}	Minimum allowable approach temperature in heat exchangers (K)
ϵ_{i-1}	Efficiency of heat transfer from effect $i-1$ to effect i (if no heat loss, $\epsilon = 1$)
X_i	Latent heat of condensation of vapor stream V_i (kJ/kg)

APPENDIX A: DETAILED DERIVATION

This detailed derivation is based on the effect shown in Figure 1.

Material balance on effect i:

$$F_i = P_i + V_i \quad (1)$$

Energy balance on effect i:

$$F_i h_{p,i} + Q_i = P_i h_{p,i} + V_i H_{v,i} \quad (2)$$

Substitute $P_i = F_i - V_i$ into (2) and rearrange:

$$Q_i = F_i (h_{p,i} - h_{F,i}) - V_i (H_{v,i} - h_{p,i}) \quad (3)$$

Because Figure 1 shows the temperature of the evaporator feed stream equal to the effect temperature, sensible heat effects are ignored. Therefore, Q_i is the amount of heat available for vaporization in effect i. Q_i can also be expressed in terms of the heat cascaded down from effect i-1, as well as other sensible heat sources and sinks in the evaporation system:

$$Q_i = (Q_{i-1,i} + q_{HU,i-1} - q_{c,i-1} + q_{ri,i}) \quad (28)$$

where:

$Q_{i-1,i}$ = the latent heat available for transfer from effect i-1 to effect i

$$Q_{i-1,i} = V_{i-1} (H_{v,i-1} - h_{c,i-1}) + V_{i-1} e_{i-1} \quad (29)$$

$q_{HU,i-1}$ = the amount of hot utilities at level i-1 added to the system

$q_{c,i-1}$ = the cold stream sensible heat requirement which is supplied by V_{i-1}

e_{i-1} = the fraction of heat not lost in transferring from effect i-1 to effect i (if $c = 1$, no heat loss)

$q_{ri,i}$ = the hot stream sensible heat surplus which is added

to effect i

Equations (28) and (29) are substituted into (3) and rearranged:

$$V_i = \frac{(V_{i-1} \lambda_{i-1} + Q_{HU_{i-1}} - q_{C_{i-1}}) \epsilon_{i-1} + q_{H_i} - F_i (h_{P_i} - h_{F_i})}{H_{V_i} - h_{P_i}} \quad (30)$$

For further manipulation, V_{i-1} must be removed from the right side of equation (30). If $i = 1$:

$$V_1 = \frac{(Q_{HU_0} - q_{C_0}) \epsilon_0 + q_{H_1} - F_1 (h_{P_1} - h_{F_1})}{H_{V_1} - h_{P_1}} \quad (31)$$

or:

$$V_1 = \frac{Q_{HU_0} \epsilon_0}{H_{V_1} - h_{P_1}} - \frac{q_{C_0} \epsilon_0 - q_{H_1} + F_1 (h_{P_1} - h_{F_1})}{H_{V_1} - h_{P_1}} \quad (32)$$

If $i = 2$:

$$V_2 = \frac{(V_1 \lambda_1 + Q_{HU_1} - q_{C_1}) \epsilon_1 + q_{H_2} - F_2 (h_{P_2} - h_{F_2})}{H_{V_2} - h_{P_2}} \quad (33)$$

Substitute (32) into (33) and rearrange:

$$V_2 = \frac{Q_{HU_0} \epsilon_0}{H_{V_2} - h_{P_2}} \cdot \frac{\lambda_1 \epsilon_1}{H_{V_1} - h_{P_1}} + \frac{Q_{HU_1} \epsilon_1}{H_{V_2} - h_{P_2}} - \frac{[q_{C_0} \epsilon_0 - q_{H_1} + F_1 (h_{P_1} - h_{F_1})]}{H_{V_1} - h_{P_1}} \cdot \frac{\lambda_1 \epsilon_1}{H_{V_2} - h_{P_2}} - \frac{q_{C_1} \epsilon_1 - q_{H_2} + F_2 (h_{P_2} - h_{F_2})}{H_{V_2} - h_{P_2}} \quad (34)$$

These expressions can be generalized for effect i :

$$\begin{aligned}
V_i = & \sum_{j=1}^i \frac{Q_{HU_{j-1}} \epsilon_{j-1}}{H_{V_j} - h_{P_j}} \prod_{k=j}^{i-1} \frac{\lambda_k \epsilon_k}{H_{V_{k+1}} - h_{P_{k+1}}} \\
& - \sum_{j=1}^i \frac{q_{C_{j-1}} \epsilon_{j-1} - q_{H_j} + F_j(h_{P_j} - h_{F_j})}{H_{V_j} - h_{P_j}} \prod_{k=j}^{i-1} \frac{\lambda_k \epsilon_k}{H_{V_{k+1}} - h_{P_{k+1}}} \quad (35)
\end{aligned}$$

The following material balance constraint forces the sum of the vapor generated in each of the N effects to be equal to the total solvent removed by vaporization, V_T .

$$V_T = \sum_{i=1}^N V_i \quad (36)$$

Substitute (35) into (36) and rearrange:

$$\begin{aligned}
\sum_{i=1}^N \sum_{j=1}^i \frac{Q_{HU_{j-1}} \epsilon_{j-1}}{H_{V_j} - h_{P_j}} \prod_{k=j}^{i-1} \frac{\lambda_k \epsilon_k}{H_{V_{k+1}} - h_{P_{k+1}}} = V_T \\
+ \sum_{i=1}^N \sum_{j=1}^i \frac{q_{C_{j-1}} \epsilon_{j-1} - q_{H_j} + F_j(h_{P_j} - h_{F_j})}{H_{V_j} - h_{P_j}} \prod_{k=j}^{i-1} \frac{\lambda_k \epsilon_k}{H_{V_{k+1}} - h_{P_{k+1}}} \quad (37)
\end{aligned}$$

In its present form, equation (37) is too cumbersome to be very useful for demonstrating our synthesis technique. Introducing assumptions such as only one hot utility, negligible heat of mixing, small boiling point elevation, and negligible heat loss yields an approximation to equation (37) which lends itself well to a simple synthesis technique.

Allow only one hot utility, Q_{HU_0} , i.e. $C_{HU_j} = 0, j = 2, N$:

$$Q_{HU_0} = L^{VT} \prod_{i=1}^N \sum_{j=1}^i \frac{q_{C_{j-1}}^{i-1} - q_{H_j} + F_j(h_{P_j} - h_{F_j})}{H_{V_j} - h_{P_j}}$$

$$\times \prod_{k=j}^{i-1} \frac{\lambda_k \epsilon_k}{H_{V_{k+1}} - h_{P_{k+1}}} \left(\sum_{i=1}^N \prod_{k=j}^{i-1} \frac{\lambda_k \epsilon_k}{H_{V_{k+1}} - h_{P_{k+1}}} \right)^{-1} \frac{V}{\epsilon_0} \quad (38)$$

If the heat of mixing is negligible, the following relation holds:

$$F_i h_{F_i} = P_i h_{P_i} + V_i h_{V_i} \quad (39)$$

Substitute (39) into (2):

$$Q_i = V_i (H_{V_i} - h_{V_i}) \quad (40)$$

or:

$$V_i \frac{q_{C_{j-1}}^{i-1} - q_{H_j} + F_j(h_{P_j} - h_{F_j})}{H_{V_j} - h_{P_j}} = \frac{V_i (H_{V_i} - h_{V_i})}{H_{V_i} - h_{V_i}} \quad (41)$$

Comparing (41) with (30) yields the simplified form of (38):

$$Q_{HU_0} = \left(V_T + \sum_{i=1}^N \sum_{j=1}^i \frac{q_{C_{j-1}}^{i-1} - q_{H_j}}{H_{V_j} - h_{V_j}} \prod_{k=j}^{i-1} \frac{\lambda_k \epsilon_k}{H_{V_{k+1}} - h_{V_{k+1}}} \right)$$

$$\times \left(\sum_{i=1}^N \prod_{k=j}^{i-1} \frac{\lambda_k \epsilon_k}{H_{V_{k+1}} - h_{V_{k+1}}} \right)^{-1} \frac{H_{V_i} - h_{V_i}}{\epsilon_0} \quad (42)$$

If the boiling point elevation is relatively small, the heats of vaporization and condensation can be assumed to be equal:

$$H_{v_j} - h_{v_j} = X_j \quad (43)$$

If the heat losses are neglected, i.e. $i_{i-1} = 1$, $i = 1, N-1$, then (43) and (42) yield:

$$Q_{HU_0} = \left(v_T - \sum_{i=1}^N \sum_{j=1}^i q_{c_j} - \sum_{k=j}^M \right) \left(\sum_{i=1}^N \prod_{k=j}^{i-1} \frac{\lambda_k}{\lambda_{k+1}} \right)^{-1} \lambda_1 \quad (44)$$

For a triple-effect system:

$$Q_{HU_0} = \left(v_T + \frac{q_{c_0} - q_{H_1}}{x_1} + \frac{q_{c_0} - q_{H_{M_1}} + q_{c_1} - q_{H_2}}{x_2} + \frac{q_{c_0} - q_{H_{N_1}} + q_{W_1} - q_{H_2} + q_{c_2} - q_{H_3}}{x_3} \right) \left(\frac{1}{\lambda_1} + \frac{1}{\lambda_2} + \frac{1}{\lambda_3} \right)^{-1} \quad (45)$$

Define:

$$q_i = H \left(\sum_{j=1}^i q_{c_j} - q_{H_i} \right) \quad (46)$$

Substitute (46) into (45):

$$Q_{HU_0} = \left(v_T + \sum_{i=1}^N \right) \left(\sum_{i=1}^N \right) \quad (47)$$

Since λ_i is not a strong function of temperature:

$$Q_{HU_0} \sim \left(v_T + \sum_{i=1}^N \frac{q_i}{\lambda_i} \right) \left(\frac{1}{N^2} \sum_{i=1}^N \lambda_i \right) \quad (48)$$

Equations (47) and (48), the steam consumption equations, are identical to equations (6) and (8), respectively.

APPENDIX B: HEURISTIC 1

Heuristic 1: The effect temperatures of the minimum utility N-effect evaporation system are contained in the minimum utility N+1-effect system.

Recall equation (8):

$$Q_{HU_0} \sim \left(v_T + \sum_{i=1}^N \frac{q_i}{\lambda_i} \right) \left(\frac{1}{N^2} \sum_{i=1}^N \lambda_i \right) \quad (8)$$

Define:

$S_N = \{T_i \mid i = 1, N\}$ = set of N effect temperatures with minimum utility use

$k = \{T_k\}$ = effect temperature added to existing minimum utility N-effect system

$S_{N+1} = \{T_i \mid i = 1, N+1\} = S_N \cup k$ = set of N+1 effect temperatures predicted by Heuristic 1

$S_{N+1}' = \{T_j \mid j = 1, N+1\}$ = set of N+1 effects with minimum utility use

$S_N' = S_{N+1}' \setminus k$

Heuristic 1 predicts that $S_N = S_{N'}$ and $S_{N+1} = S_{N < M'}$. However, if the heuristic fails:

$$Q_{HJ_0}^{IS} J < \wedge V \quad (49>$$

and:

$$Q_{HU_0}(S_{N+1}') < Q_{HU_0}(S_{N+1}) \quad (50)$$

From (8):

$$Q_{HU_0}(S_N) \sim \left(v_T + \sum_{i \in S_N} \frac{q_i}{\lambda_i} \right) \left(\frac{1}{N^2} \sum_{i \in S_N} \lambda_i \right) \quad (51)$$

and:

$$Q_{HU_0}(S_{N'}) \sim \left(v_T + \sum_{i \in S_{N'}} \frac{q_i}{\lambda_i} \right) \left(\frac{1}{N^2} \sum_{i \in S_{N'}} \lambda_i \right) \quad (52)$$

From the above definitions:

$$Q_{HU_0}(S_{N+1}') = Q_{HU_0}(S_{N'} \cup k) \\ = \left(v_T + \sum_{i \in S_{N'}} \frac{q_i}{\lambda_i} + \frac{q_k}{\lambda_k} \right) \left(\frac{1}{N^2} \sum_{i \in S_{N'}} \lambda_i + \lambda_k \right) \quad (53i)$$

and:

$$Q_{HU_0}(S_{N+1}) = Q_{HU_0}(S_N \cup k)$$

$$\frac{1}{k} \sum_{i \in S_N} x_i \bar{M}_i / \sqrt{v_i} \quad (54)$$

$$\frac{1}{k} \sum_{i \in S_N} x_i \bar{M}_i / \sqrt{v_i}$$

Subtract (54) from (53):

$$Q_{H U J} S_{N+1} - Q_{H U} \langle S_{N+1} \rangle - (-N - r \wedge V \wedge H U J V - Q_{H U J} S_N)$$

$$+ \lambda_k \left(\sum_{i \in S_N} \frac{q_i}{\lambda_i} - \sum_{i \in S_N} \frac{q_i}{\lambda_i} \right)$$

$$+ \frac{q_k}{\lambda_k} \left(\sum_{i \in S_N} \lambda_i - \sum_{i \in S_N} \lambda_i \right) \quad (55)$$

If Heuristic 1 fails, equation (55) will have a negative value. Note that the entire equation is divided by $(N + 1)^2$, so as N increases the potential error decreases. In addition, the first term in equation (55) is multiplied by IN^2 , while the remaining terms are not. This term is always positive and in most cases will dominate the other two terms. In other words, the last two terms must have large negative values before Heuristic 1 can be violated. The authors have yet to encounter a violation of this heuristic.

APPENDIX C: HEURISTIC 2

Heuristic 2: An evaporation feed stream, in following the most direct path from feed temperature to product temperature without bypass, should enter any effect in its path that does not already have a feed stream. Restated: do not skip an effect which is being approached for the first time.

This heuristic is justified by constructing appropriate Detailed Effect Temperature Diagrams for four cases: (a), hot feed skipping effect i , (b), hot feed entering effect i without skipping, (c), cold feed skipping effect i , and (d), cold feed entering effect i . For simplicity, vaporization is assumed to be equal in all effects. In addition, boiling point elevation is neglected. This omission does not alter the results in any way, but merely makes the four cases easier to illustrate. Figures 18, 19, 21, and 22 show Cases (a) through (d), with the temperature scale extending from effect $i-1$ to effect M . The temperature intervals are numbered from $j-1$ to $j+2$, with process stream heat loads included for each interval ($q_{PROC, k} = j-1, j+2$). In each case, temperature interval j is the interval of interest.

HOT FEED

Case (a) is illustrated in Figure 18. Hot feed (flowrate = $P \cdot mV$) skips effect i , feeding effect $i+1$ instead. Cold feed (flowrate = $P \cdot \epsilon V$) from an effect below $i+1$ is shown on the cold side of the diagram. This stream feeds effect i , generating vapor (flowrate = V) and product (flowrate = $P \cdot (\epsilon - 1)V$). Also shown in Figure 18 are the condensed vapor streams from effect $i-1$ and above (flowrate = $(i-1)V$). Direct heating takes place only at effect $i+1$, while all other sensible heat loads are recorded in the indirect column.

Case (b) is shown in Figure 19. The hot feed stream (flowrate = $P \cdot mV$) enters effect i , generating vapor (flowrate = V) and product (flowrate = $P \cdot (m - 1)V$). This product in turn becomes the feed for effect $i+1$. In Case (b), the cold product stream does not enter effect i because it was already fed by the hot feed. The flowrate of the cold feed stream is $P \cdot \epsilon V$ minus the amount of vapor removed previously in effect i . Its flowrate is then $P \cdot (\epsilon - 1)V$. Direct heating takes place in both effect i and $i+1$, with all other sensible heat loads recorded in as indirect heat. Except for the feeding of effect i , Cases (a) and (b) are identical.

Comparing Figures 18 and 19 shows that except for temperature interval j , all other net heat loads are equal. Note that in interval $j+2$, the q_{DIR} and q_{IND} differ from Case (a) to Case (b). However, since these differences cancel out, the q_{MERGE} values for each case would be equal. Since this portion of the exercise is intended to demonstrate whether or not hot feed should skip effect i , the only quantity of interest is the difference between the heat loads of Cases (a) and (b), as reflected by interval j . In other words, how does skipping of effect i impact on the accumulated sensible heat requirement (q_i of that effect? In addition, how does this impact on other effects in the system (q_{i-1} , q_{i+1} , etc.)?

Interval j is within ΔT_{min}^{HX} of effect temperature T_i . Therefore, the following relation holds:

$$\text{if } q_{IND_j} \geq 0, \quad q_{MERGE_j} = q_{DIR_j} + q_{IND_j} \quad (56)$$

$$\text{if } q_{IND_j} < 0, \quad q_{MERGE_j} = q_{DIR_j} \quad (57)$$

If q_{IND_j} is non-negative, the process streams in the interval just above effect i require heat. This heat must be supplied by effect $i-1$, not effect i . Therefore, q_{IND_j} must be included in q_{MERGE_j} , thus reducing the amount of heat available to effect i . This condition corresponds to equation (56).

On the other hand, if q_{IND_j} is negative, a process heat source exists within ΔT_{min}^{HX} of effect i . This heat cannot be transferred to effect i because doing so would violate the minimum approach temperature. Therefore, it must be cascaded to the next level. The only sensible heat available to effect i in interval j is q_{DIR_j} . This is shown in equation (57).

Referring to Figure 18:

$$q_{DIR_j} = 0 \quad (58)$$

$$SND_j = -(m + i - \ell - 1)FC_V A'' C + W : \quad (59)$$

$$q_{MERGE_j} = q_{DIR_j} + q_{IND_j}$$

$$= -(m + i - \ell - 1)FC_V A'' C + q_{PROC_j} \quad (60)$$

and:

$$W_j \geq (m + i - \ell - 1)FC_V \Delta T_{min}^{HX} \quad (61)$$

On the other hand, if $q_{IND_j} < 0$:

$$q_{MERGE_j} = q_{DIR_j} = 0 \quad (62)$$

and:

$$W_j < (m + i - \ell - 1)FC_V \Delta T_{min}^H \quad (63)$$

For Case (b) Figure 19 shows:

$$q_{DIR_j} = -(FC_P + mFC_V) A T \Delta \quad (64)$$

$$q_{IND_j} = t^A C_p - (i - C)FC_V JAT_{min} \cdot A_{PROC} \quad (65)$$

If $q_{IND_j} \geq 0$:

$$q_{MERGE_j} = q_{DIR_j} + q_{IND_j}$$

$$= A m \cdot i - (FC_P + mFC_V) A T \Delta + q_{PROC_j} \quad (66)$$

and:

$$W_j \geq (FC_P + mFC_V) A T \Delta \quad (67)$$

If $SND_j < 0$:

$$q_{MERGE_j} = q_{DIR_j} = -(FC_P + mFC_V) A T \Delta \quad (68)$$

and:

$$q_{PROC_j} < -[FC_p - (i - 1)FC_w] \quad (69)$$

Recall that except for interval j , all other net heat load terms for both cases are identical. Therefore, subtracting q_{MERGE_i} for Case (b) (non-skipping) from q_{MERGE_j} for Case (a) (skipping) yields the difference between their respective q_i values. These Aq_i values vary with $q_{DDOR_{ROC_j}}$ as follows:

$$\Delta q_i = FC_V \Delta T_{min}^{HX} > 0 \quad \text{when} \quad W_i < m \cdot i - \epsilon - DFC_V AT_n \quad (70)$$

$$Aq_i = (m \cdot i - \epsilon) FC_V AT_n - q_{PROC_j} > 0 \quad \text{when} \quad (m \cdot i - \epsilon - DFC_V AT_n) > q_{PROC_j} - [FC_p - (i - \epsilon) FC_w] AT_{min} \quad (71)$$

$$Aq_i = (FC_D \cdot m FC_w) AT_{min}^{HX} > 0 \quad \text{when} \quad q_{PROC_j} < -[FC_p - (i - \epsilon) FC_w] AT_{min}^{HX} \quad (72)$$

The above three equations show that it is never beneficial for hot feed to skip an effect. Whenever this skipping occurs, the steam use of the system will increase, which we refer to as a "heat loss." The amount of heat lost by skipping depends upon the magnitude of the process heat available in interval j . If the process streams act as a large heat sink ($q_{PROC_j} \ll 0$) the heat loss incurred by skipping effect i is $FC_V AT_n$. On the other hand, if the process streams act as a large heat source ($q_{DDOR_{ROC_j}} \ll 0$), the loss is $(FC_D \cdot m FC_w) AT_{min}^{HX}$. In any event, when a hot feed stream skips an effect, a heat loss results.

In addition to the heat loss at effect i , all effects from $i+1$ through $N-1$ also experience heat loss. If one were to calculate q_{i+1} for both Figures 18 and 19, Aq_{j-M} would be $FC_V AT_n$. This heat loss is not gained back until effect N , as illustrated in Figure 20. Figure 20a and Figure 20b show effect N for Cases (a) and (b), respectively. The net difference between the two is:

$$\Delta q_{DIR_N} = -FC_V \Delta T_{min}^{HX} \quad (73)$$

As shown in the steam consumption equations, any surplus or deficit of heat in the evaporation system is distributed among all N effects. Therefore, the difference in the steam consumption (ΔQ_{HU_0}) of a system with skipping versus one without skipping is approximated by adding all heat losses together and dividing by N:

$$\left(\frac{N-i}{N} \right) FC_V \Delta T_{min}^{HX} \leq \Delta Q_{HU_0} \leq \frac{[FC_P + (N+m-i-1)FC_V] \Delta T_{min}^{HX}}{N} \quad (74)$$

COLD FEED

A similar argument can be developed to compare Case (c), cold feed skipping effect i, with Case (d), cold feed entering effect i. Shown in Figures 21 and 22 are Cases (c) and (d), respectively. Once again our attention is focused on temperature interval j.

In Figure 21, the cold product from effect i+1 (flowrate = $P + (m-1)V$) skips effect i. Hot product (flowrate = $P + \ell V$) from effect i-1 or above enters effect i, giving rise to a direct heating term in interval j.

In Figure 22, the cold product from effect i+1 enters effect i, yielding product with a flowrate of $P + (m-2)V$. Consequently, the hot product from effect i-1 or above has a smaller flowrate ($P + (\ell-1)V$) than in Figure 21. No direct heating takes place in Case (d).

From Figure 21:

$$q_{DIR_j} = -(FC_P + \ell FC_V) \Delta T_{min}^{HX} \quad (75)$$

$$q_{IND_j} = [FC_P + (m-i)FC_V] \Delta T_{min}^{HX} + q_{PROC_j} \quad (76)$$

If $q_{IND_j} \geq 0$:

$$\begin{aligned}
 q_{\text{MERGE}_j} &= q_{\text{DIR}_j} + q_{\text{IND}_j} \\
 &= (m - i - \ell)FC_V \Delta T_{\text{min}}^{\text{HX}} + q_{\text{PROC}_j}
 \end{aligned}
 \tag{77}$$

and:

$$q_{\text{PROC}_j} \geq -[FC_p + (m - i)FC_V] \Delta T_{\text{min}}^{\text{HX}} \tag{78}$$

If $q_{\text{IND}_j} < 0$:

$$q_{\text{MERGE}_j} = q_{\text{IND}_j} - (FC_p + FC_V) \Delta T_{\text{min}}^{\text{HX}} \tag{79}$$

and:

$$q_{\text{PROC}_j} < -FC_p + (m - i)FC_V \Delta T_{\text{min}}^{\text{HX}} \tag{80}$$

From Figure 22:

$$q_{\text{DIR}_j} = 0 \tag{81}$$

$$q_{\text{IND}_j} = (m - i - \ell + 1)FC_V \Delta T_{\text{min}}^{\text{HX}} + q_{\text{PROC}_j} \tag{82}$$

If $q_{\text{IND}_j} \geq 0$:

$$\begin{aligned}
 q_{\text{MERGE}_j} &= q_{\text{DIR}_j} + q_{\text{IND}_j} \\
 &= (m - i - \ell + 1)FC_V \Delta T_{\text{min}}^{\text{HX}} + q_{\text{PROC}_j}
 \end{aligned}
 \tag{83}$$

and:

$$q_{\text{PROC}_j} \geq -(m - i - \ell + 1)FC_V \Delta T_{\text{min}}^{\text{HX}} \tag{84}$$

If $W_j < 0$:

$$q_{\text{MERGE}_j} \leq W_j \tag{85}$$

and:

$$q_{\text{PROC}_j} < -(m - i - \ell + 1)FC_V \Delta T_{\text{min}}^{\text{HX}} \tag{86}$$

Once again, subtracting Q_{MERGE}^j for Case (d) (non-skipping) from Q_{MERGE}^j for Case (c) (skipping) yields the following values for Aq_i :

$$Aq_i = -FC_w AT_{mm}^{HX} < 0 \text{ when } q_{PROC_j} > (m - i - 1) * DFC_v AT_{mm}^{HX} \quad (87)$$

$$Aq_i = (m - i - 1) * FC_v AT_{mm}^{HX} - q_{PROC_j} < 0 \text{ when } (m - i - 1) * FC_v AT_{mm}^{HX} > q_{PROC_j} + [FC_p * (m - i) FC_w] AT_{mm}^{HX} \quad (88)$$

$$Aq_i = - (FC_p * FC_w) AT_{mm}^{HX} < 0 \text{ when } q_{PROC_j} < - [FC_p * (m - i) FC_w] AT_{mm}^{HX} \quad (89)$$

From this analysis, it appears that cold feed should indeed skip effect i in order to gain the benefit of direct heating. However, before drawing any conclusions, the impact of skipping on effect 1 must be addressed.

Figure 23 shows effect 1 for the two cases, with Figures 23a and 23b representing Cases (c) and (d), respectively. Comparing the two:

$$Aq_i = FC_w AT_{min}^{HX} \quad (90)$$

We now see that cold feed skipping effect i causes q_i through q_{i-1} to be increased by $FC_w AT_{mm}^{HX}$. With this information, the above values for Aq_i are corrected:

$$Aq_i = 0 \text{ when } q_{HUL_j} > (m - i - 1) * FC_v AT_{mm}^{HX} \quad (91)$$

$$Aq_i = (m - i - 1) * DFC_v AT_{mm}^{HX} - q_{PROC_j} < 0 \text{ when } (m - i - 1) * FC_v AT_{mm}^{HX} > q_{PROC_j} + [FC_p * (m - i) FC_w] AT_{mm}^{HX} \quad (92)$$

$$Aq_i = - [FC_p * (m - i) FC_w] AT_{mm}^{HX} < 0 \text{ when } q_{PROC_j} < - [FC_p * (m - i) FC_w] AT_{mm}^{HX} \quad (93)$$

$$\Delta q_k = FC_w AT_{min}^{HX} \quad k = 1, i-1 \quad (94)$$

Since all sensible heat gains and losses are distributed throughout the system, the overall difference in steam consumption has the following range:

$$\frac{j_{HX} \Delta T_{min}}{N} \leq \Delta U_{HU_0} \leq \left(\frac{i-1}{N} \right) FC_V \Delta T_{min}^{HV}$$

It is conceivable that skipping of an effect i could be beneficial if the effect is near effect 1 and if a large sensible heat source exists just above the effect ($q_{i-1} > C_0$). In that case, the potential gains in direct heating in effect i could outweigh the additional $FC_V AT_{mJn}^{HX}$ applied to q_1 through q_{i-1} . Except for this relatively unlikely situation, skipping with cold feed is not recommended.

Table 1: Example Problem Specifications

Feed flowrate $F = 10.0$ kg/s
 Feed concentration $X_F = 0.200$ kg solute/kg solution
 Feed temperature $T_F = 375$ K

 Product concentration $X_P = 0.400$ kg solute/kg solution
 Product temperature $T_P = 415$ K

 Heat of vaporization λ (kJ/kg) = $3270 - 2.737T$, T [=] K
 Heat capacity (kJ/kg) = $4.20 - 3.00X$, X [=] mass fraction solute
 Maximum allowable concentration $X_{\max} = 0.500$ kg solute/kg solution
 Boiling point elevation BPE = 5 K
 Evaporator heat transfer coefficient U (W/m²-K) = $8.52(T + \text{BPE}) - 1440$
 Lowest allowable normal-boiling temperature of an effect $T_{\text{low}} = 330$ K

$\Delta T_{\min}^{\text{EV}}$ for evaporators = 30 K

$\Delta T_{\min}^{\text{HX}}$ for heat exchangers = 10 K

Utilities:

Steam available at 450 K
 Cooling water available at 305 K

Process streams:

Label	Heat capacity flowrate (kW/K)	T_{in} (K)	T_{out} (K)
H1	25.0	425	360
C1	20.0	340	400

Additional information inferred from the above data:

Feed heat capacity = 3.60 kJ/kg-K
 Feed heat capacity flowrate $FC_F = 36$ kW/K
 Product flowrate = 5.0 kg/s
 Product heat capacity = 3.00 kJ/kg-K
 Product heat capacity flowrate $FC_P = 15$ kW/K
 Vapor generated = 5.0 kg/s
 Vapor concentration = 0.0 kg solute/kg solution
 Vapor heat capacity = 4.20 kJ/kg-K
 Vapor heat capacity flowrate $FC_{V_T} = 21$ kW/K

Table 2: Effect Temperature Selection Summary

	T_i (K)	X_i (kJ/kg)	Original q_i (kW) Estimate	Improved q_i (kW) Estimate
Effect 1	415	2134	-50	0
Effect 2	365	2271	-80	-30
Effect 3	330	2367	-665	-665

Table 3: Summary of Triple-Effect Flowpattern Selection

Flowpattern	Q_{HU0} (kW)	Number of U-Turns	Effect Skipped
123	3752	2	-
132	3838	2	2
213	3794	3	-
231	3706	2	-
312	3802	3	2
321	3760	2	2

Table 4: Incremental Costs of Evaporators and Heat Exchangers

A (m ²)	$\frac{\partial C}{\partial A}$ <\$/m ²)			
	Vertical Evaporator	Horizontal Evaporator	U-Tube Exchanger	Fixed-Tube-Sheet Exchanger
5	8350	5570	1380	1300
10	6030	4020	1080	1020
50	2850	1890	616	580
100	2040	1360	483	455
500	960	639	275	259

Table 5: Convergence to Equal Effect Areas

Iteration Number	Actual Effect Temperatures (K)	Flow-pattern	Steam Required (kW)	Area 1 (m ²)	Area 2 (m ²)	Area 3 (m ²)
1	420.0, 370.0, 335.0	231	3766	57.7	43.5-44.2	75.S-S3.5
2	417.3, 379.6, 335.0	321	3751	54.2	57.1-61.2	49.7-59.8
3	418.3, 378.8, 335.0	321	3756	55.8	54.5-58.1	51.1-61.3

Table 6: Flowsheet Cost Comparison

	Annual Cost (\$1000)*		
	Utilities Cost	Capital Cost	Total Cost
Min. Utility Flowsheet (Figure 15)	404	470	874
Equal Area Min. Utility (Figure 16)	413	445	858
Equal Area Non-Integrated (Figure 17)	482	421	903

*The cost of utilities and capital were calculated with the following data: annual steam cost = \$90/kW, annual cooling water cost = \$17/kW. The cost of evaporators and heat exchangers was based on the method of Guthrie [2]. These costs represent a tax credit of 48 percent on utilities and a payback period of 2.5 years on all capital equipment.

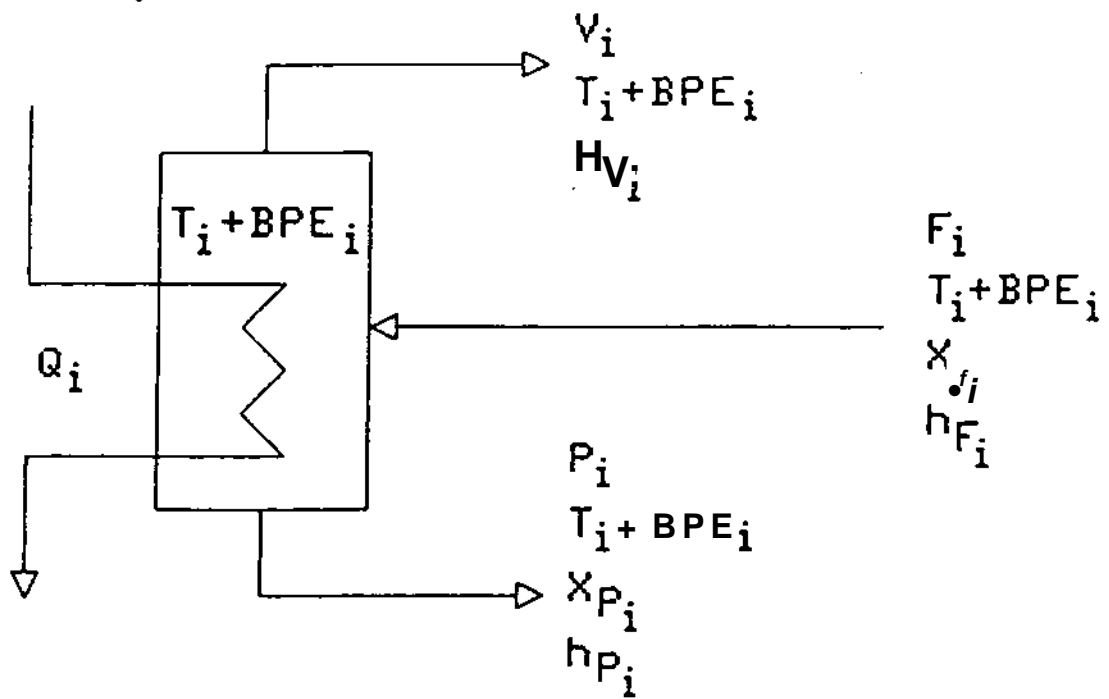


Figure 1: Effect i of an N -Effect Evaporator Sequence

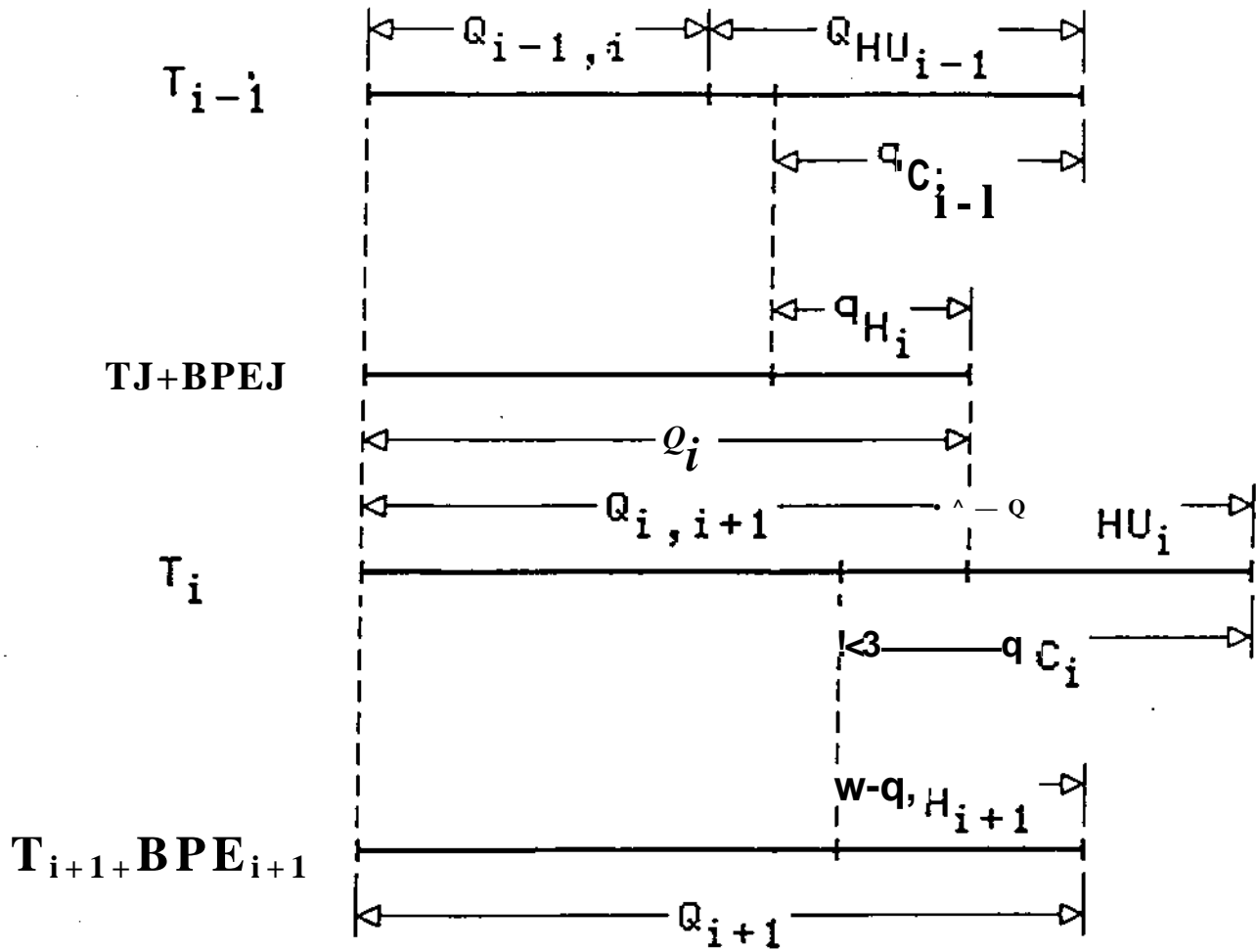


Figure 2: Graphical Representation of the Evaporator Energy Balances

		T_H	T_C	Stream Sensible Heats* (kW)	
		450	440	0	0
	HI	425	415	-150	-150
		410	400	•250	•100
		385	375	-50	•50
	V _T	375	365	-390	-340
		360	350	-10	-350
		350	340	-315	-665
		335	325	0	-665
		330	320		
FC _i	25 21			15 20	

Figure 3: Evaporation System Problem Table

(•) implies that the streams require heat from the evaporation process: (-) implies that the streams supply heat to the evaporation process. Units: T [=] K and FC [=] kW/K.

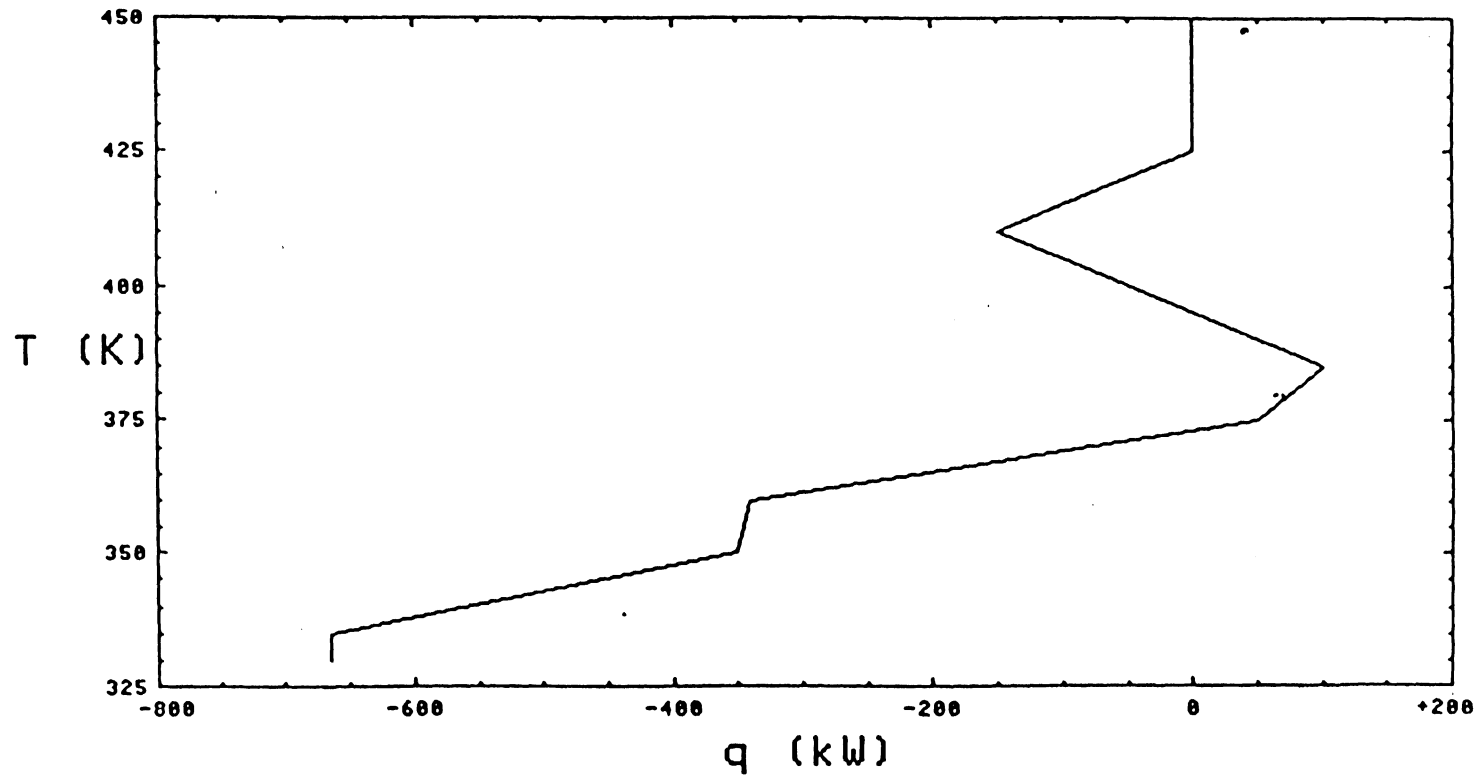


Figure 4: Accumulated Sensible Heat (q) Profile

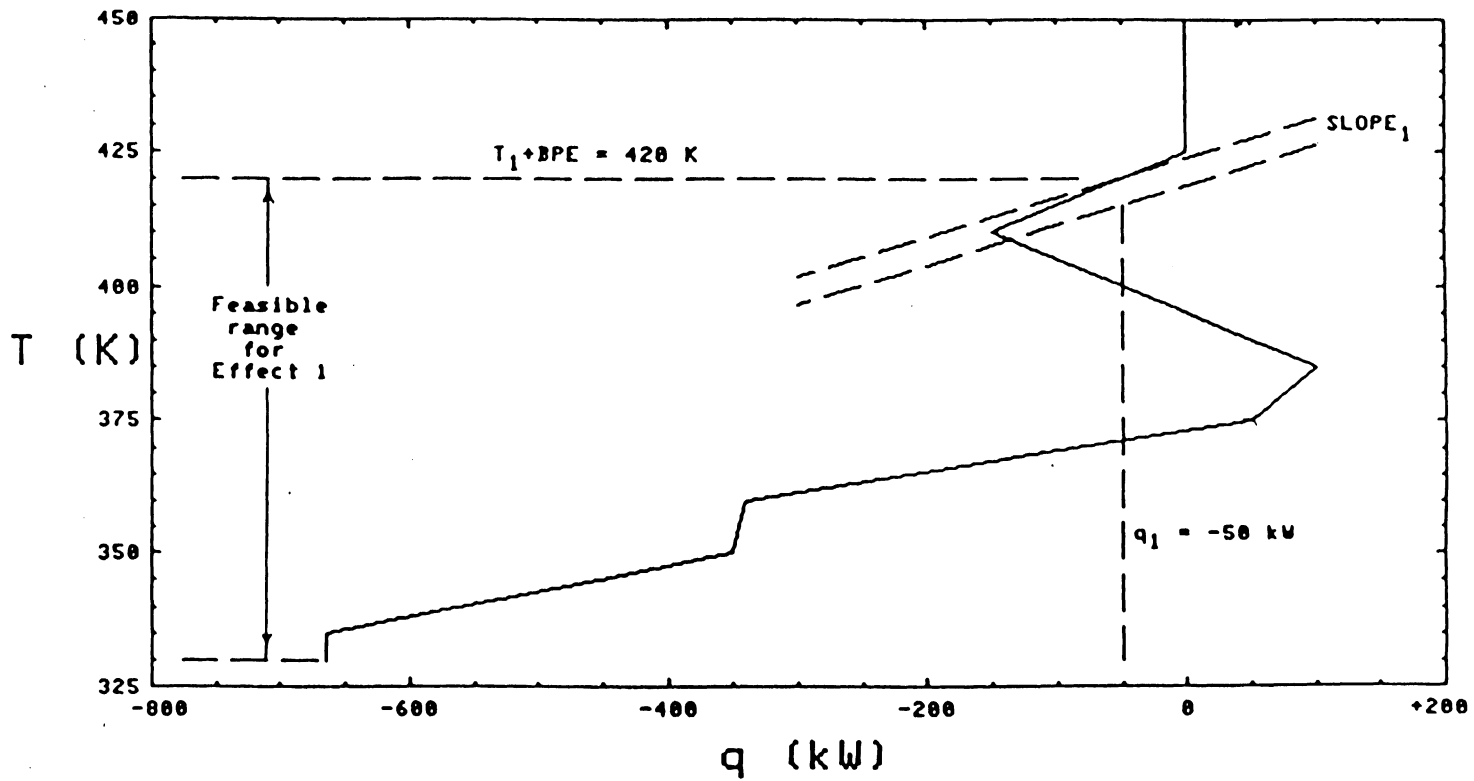


Figure 5: Selection of the First Effect Temperature

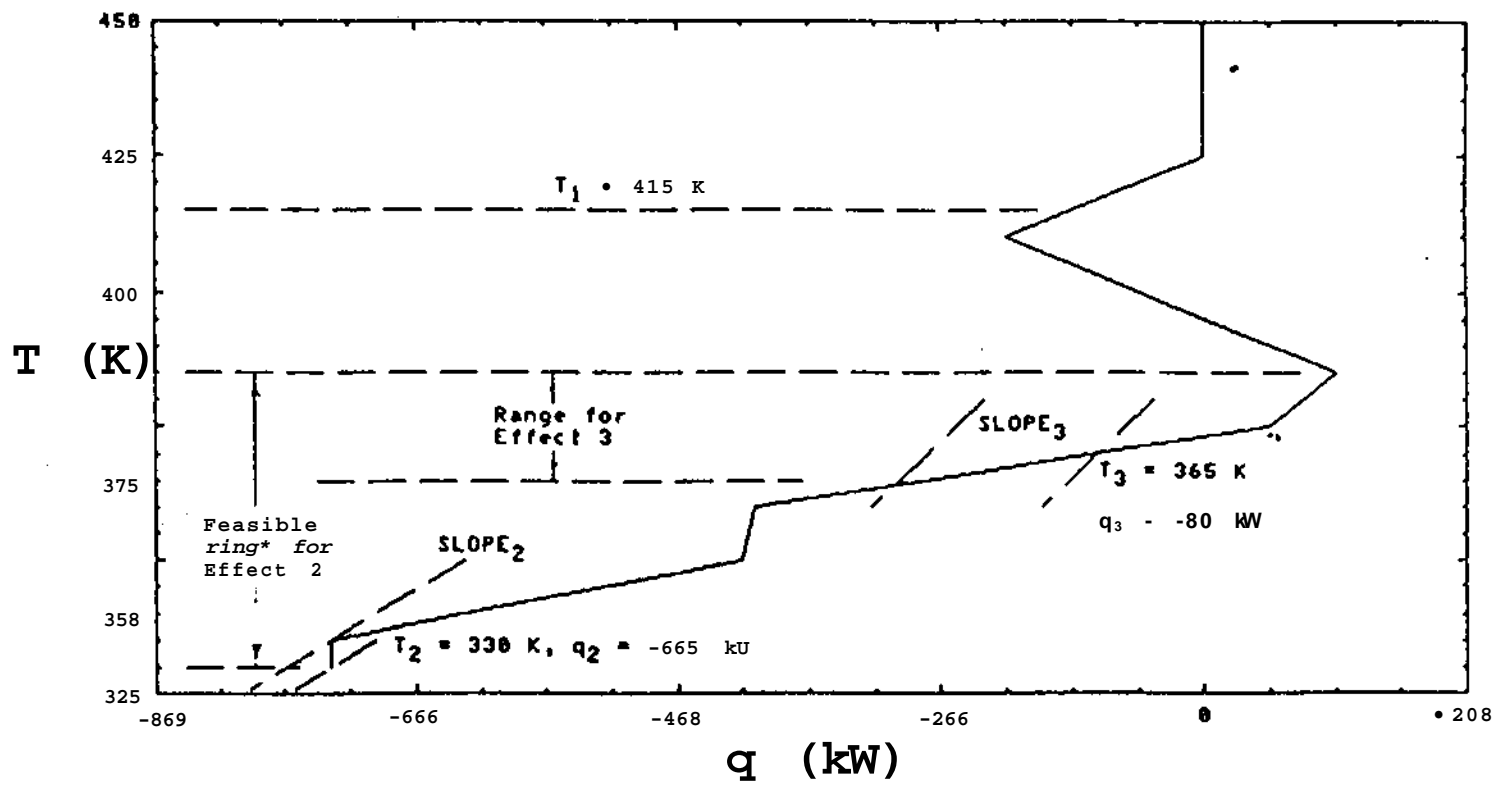


Figure 6: Selection of Remaining Effect Temperatures

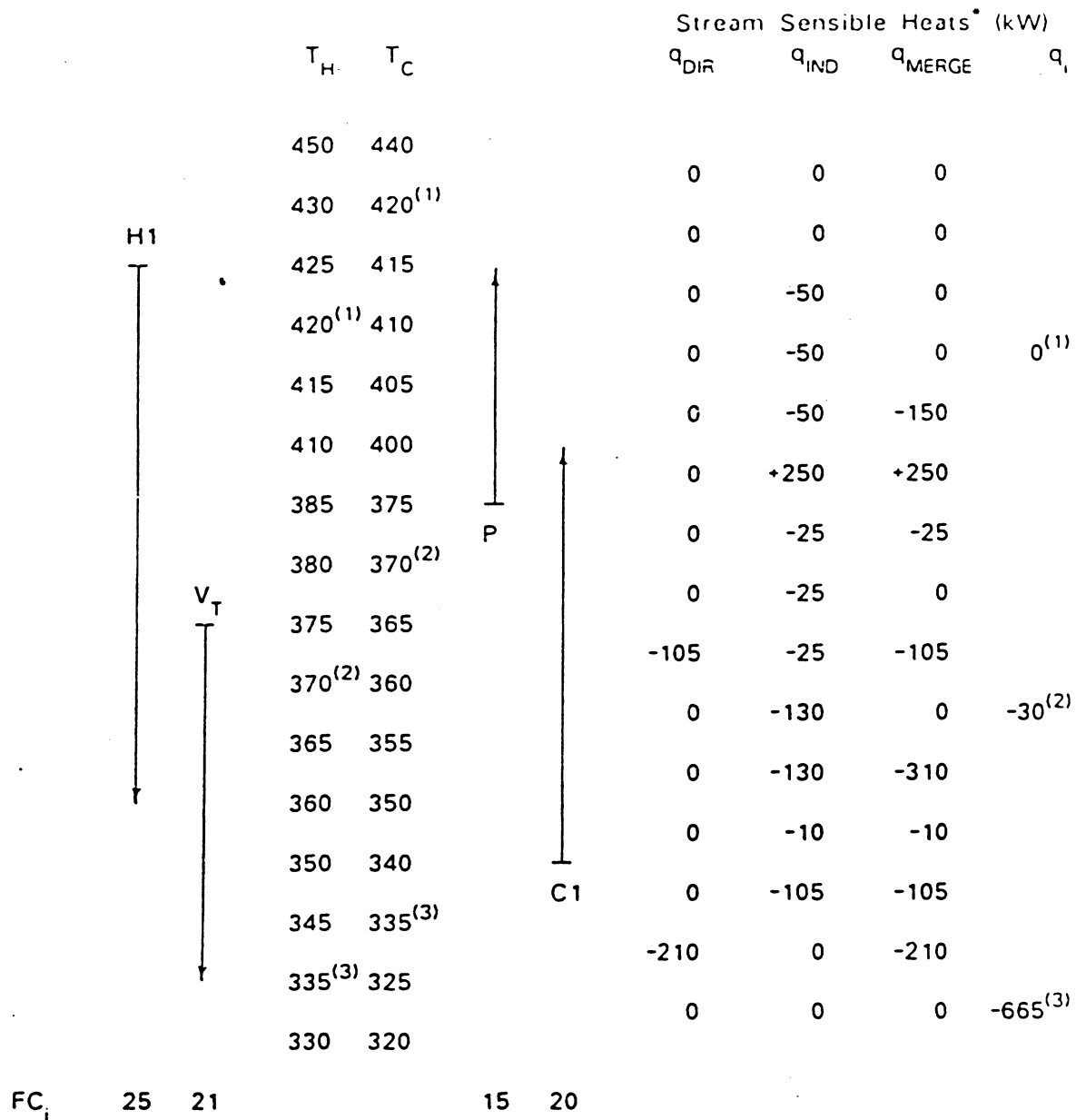


Figure 7: Preliminary Effect Temperature Diagram

* (+) implies that the streams require heat from the evaporation process; (-) implies that the streams can supply heat to the evaporation process. The numbers (1), (2), and (3) denote the actual effect temperatures and their corresponding q_i values. Units: T [=] K and FC [=] kW/K.

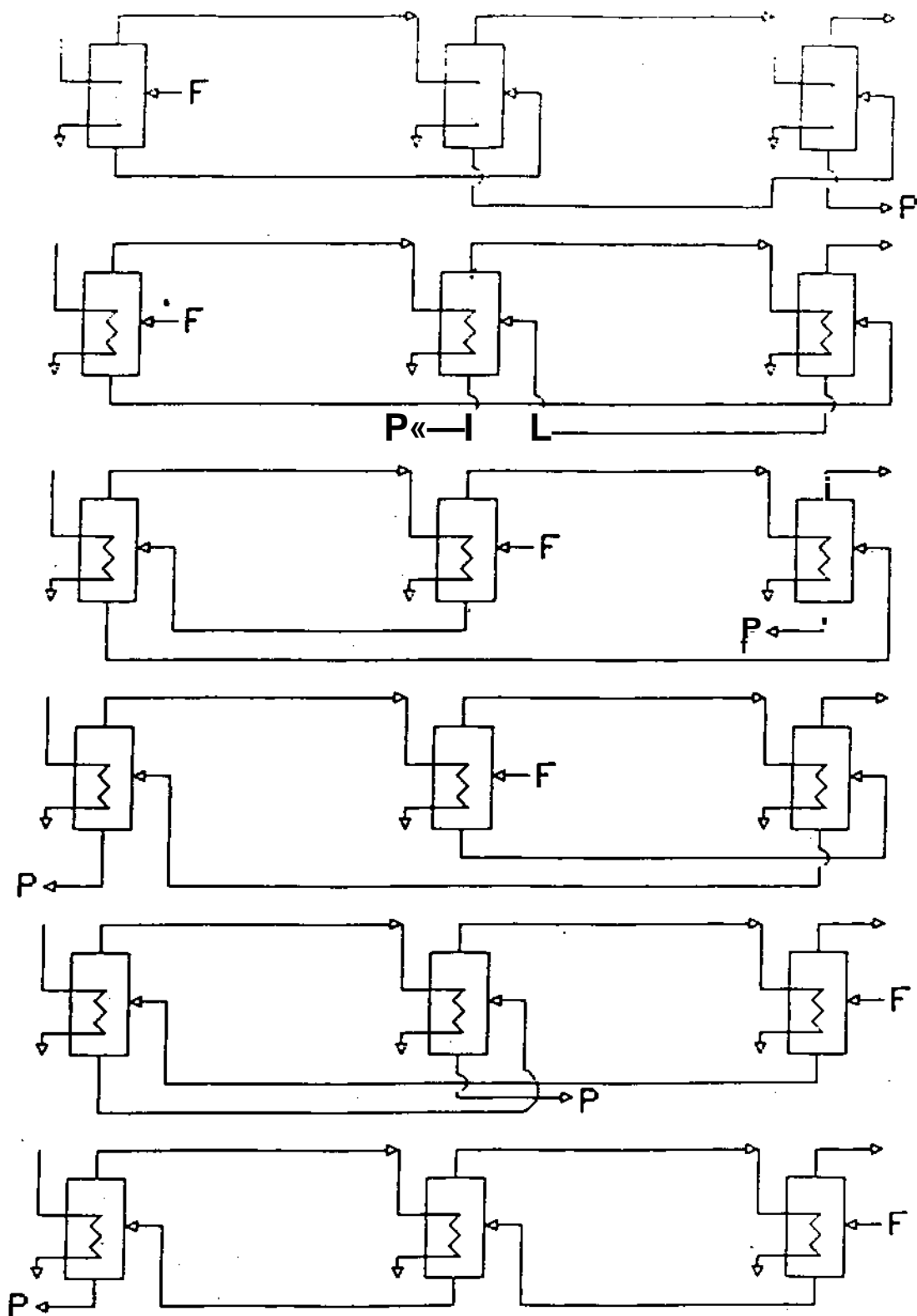


Figure 8: Triple-Effect Flowpatterns

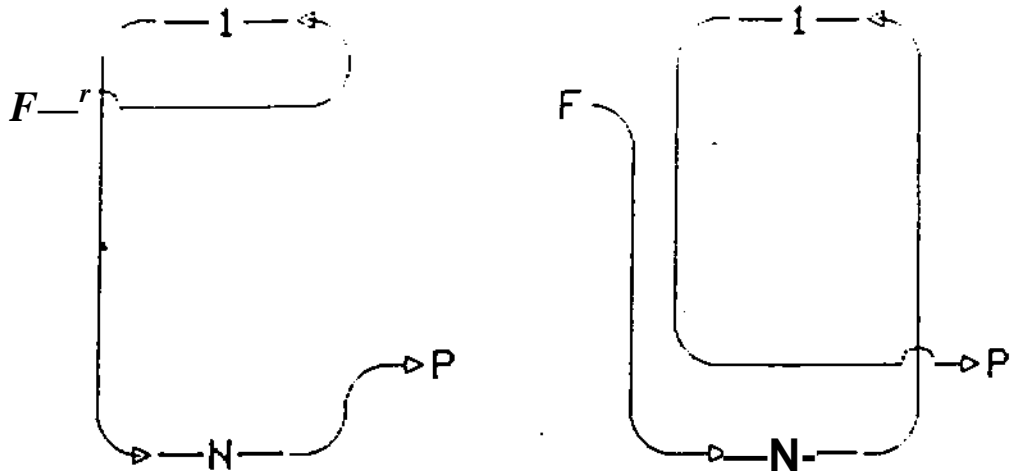


Figure 9: Evaporator Stream Overlap for Two Methods of Feeding

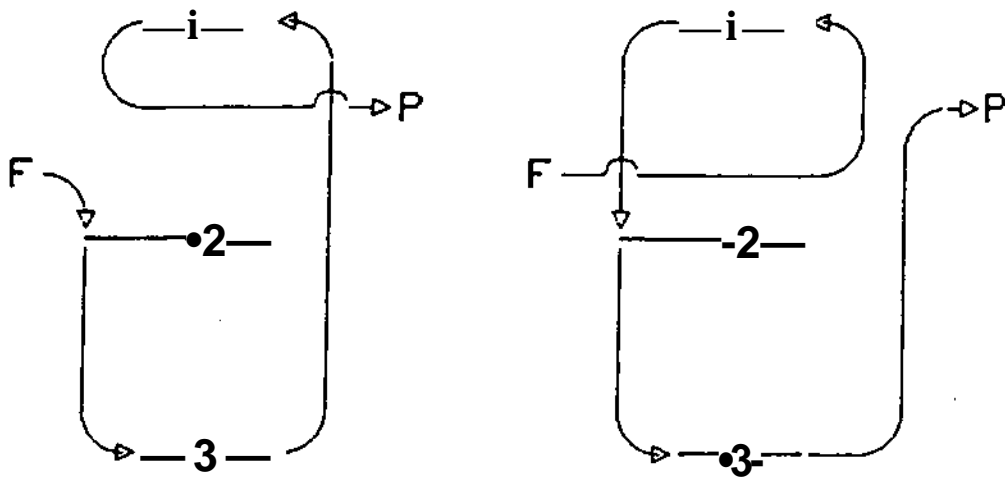


Figure 10: Comparison of Flowpatterns 123 and 231

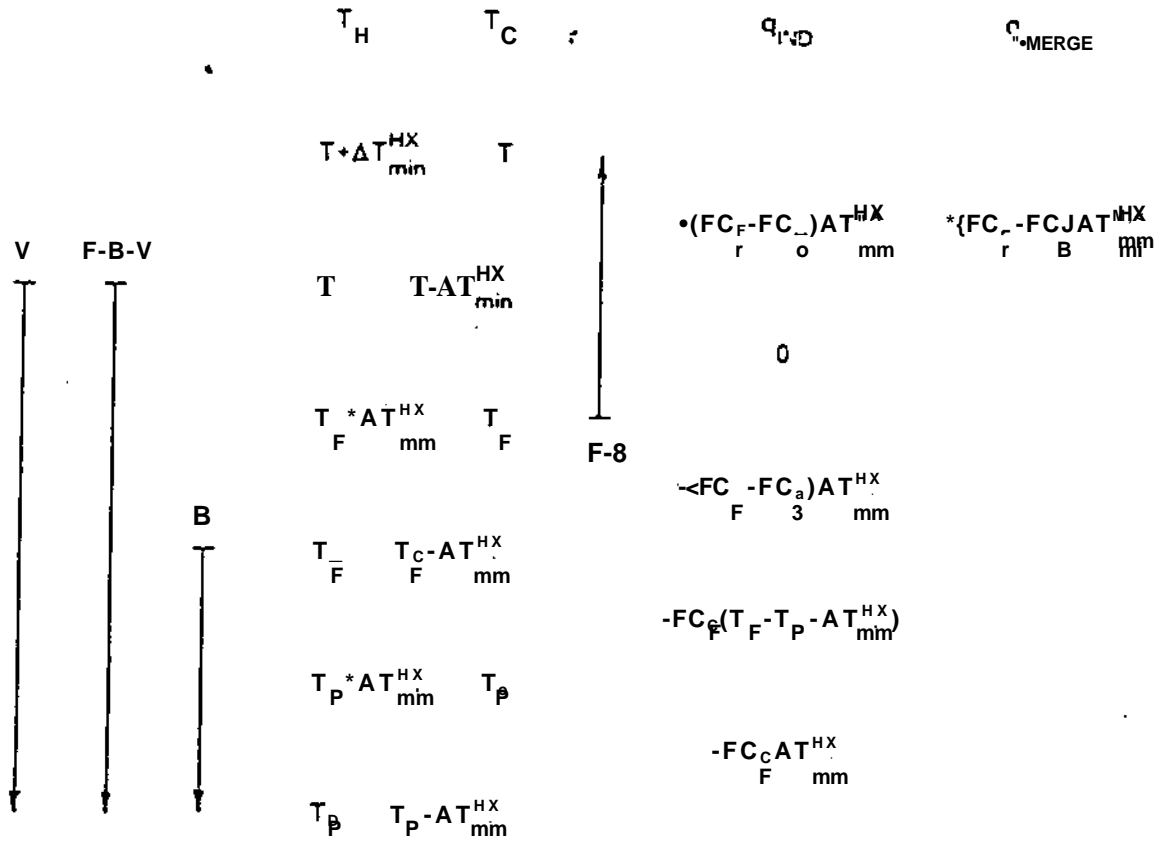


Figure 11: Typical Bypass Calculation

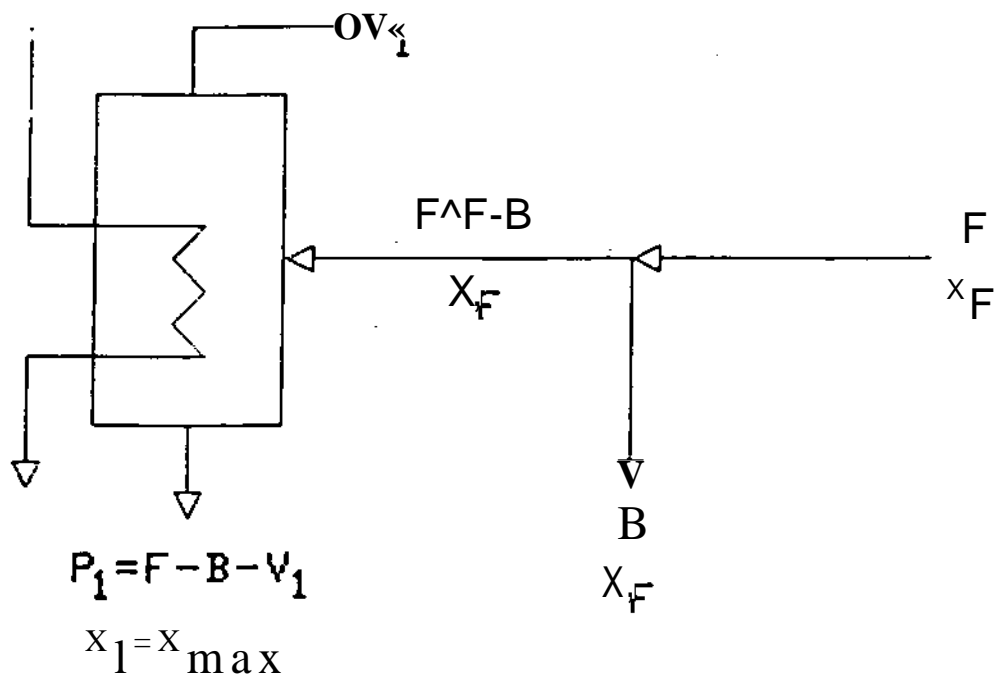


Figure 13: Evaporator Bypass of Effect 1

		Q_{HU_0}	HI.3	HI.4
		3663	125	125
Q_{V_1}	3610	3610	I	I
$\bullet V^2$	51	51	I	I
F_{r^3}	51	2	49	I
P.3	75		75	I
$F_{i,4}$	51		1	50
P.4	75			75

Figure 14: Tableau for Partition 1*

* "I" indicates the match in this cell is infeasible.

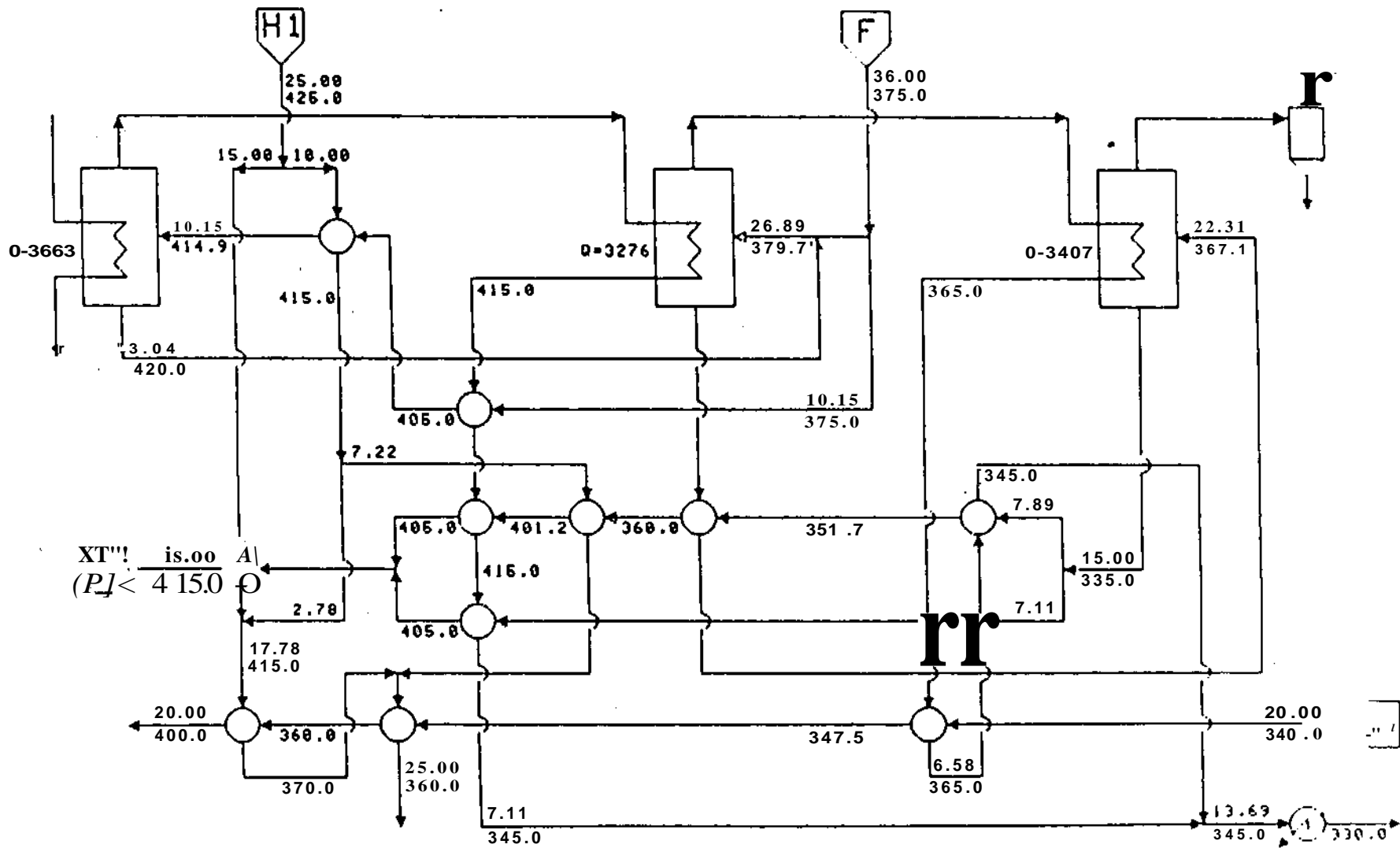


Figure 15: Minimum Utility Triple-Effect Evaporation System

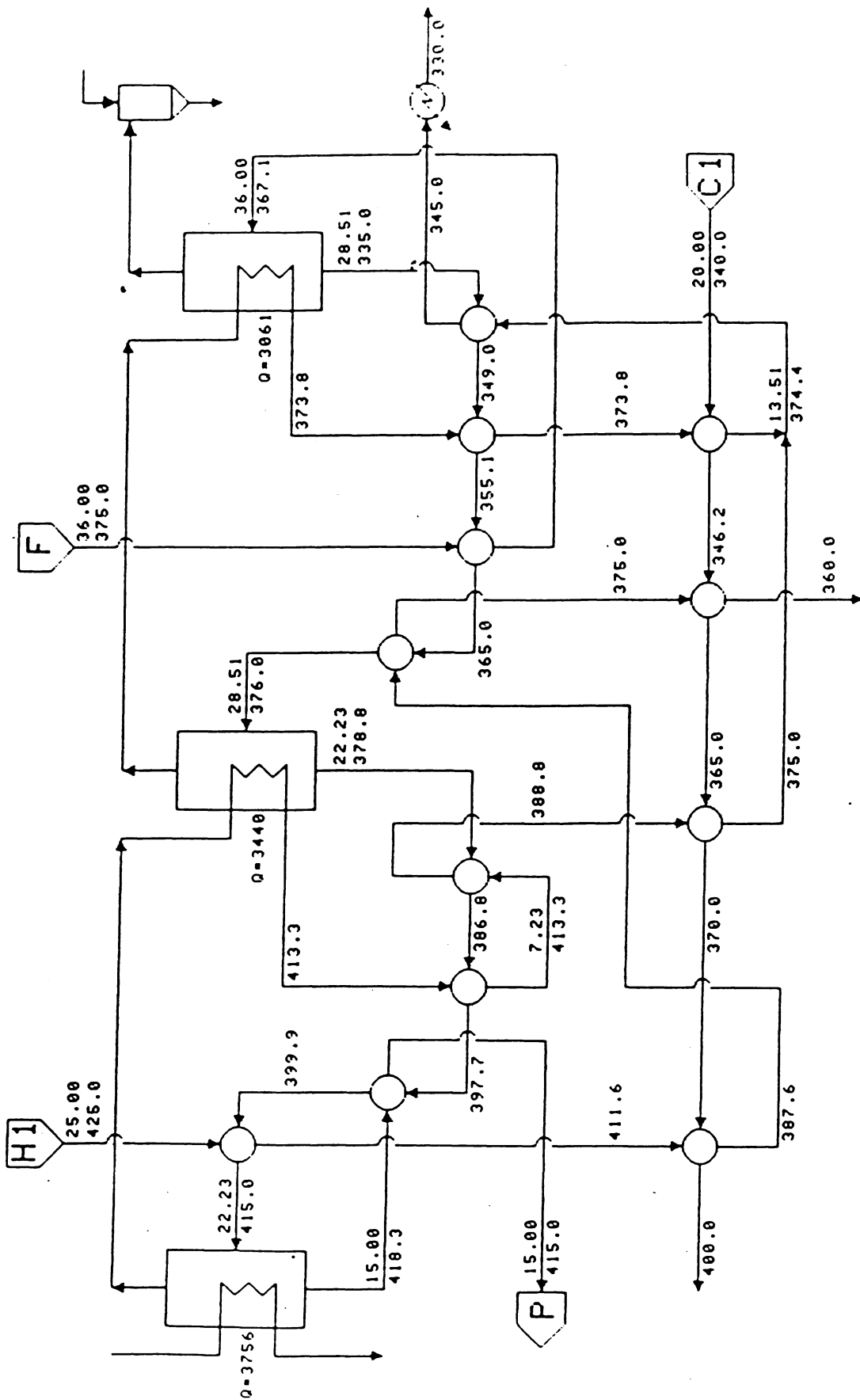


Figure 16: Minimum Utility Triple-Effect System with Equal Areas

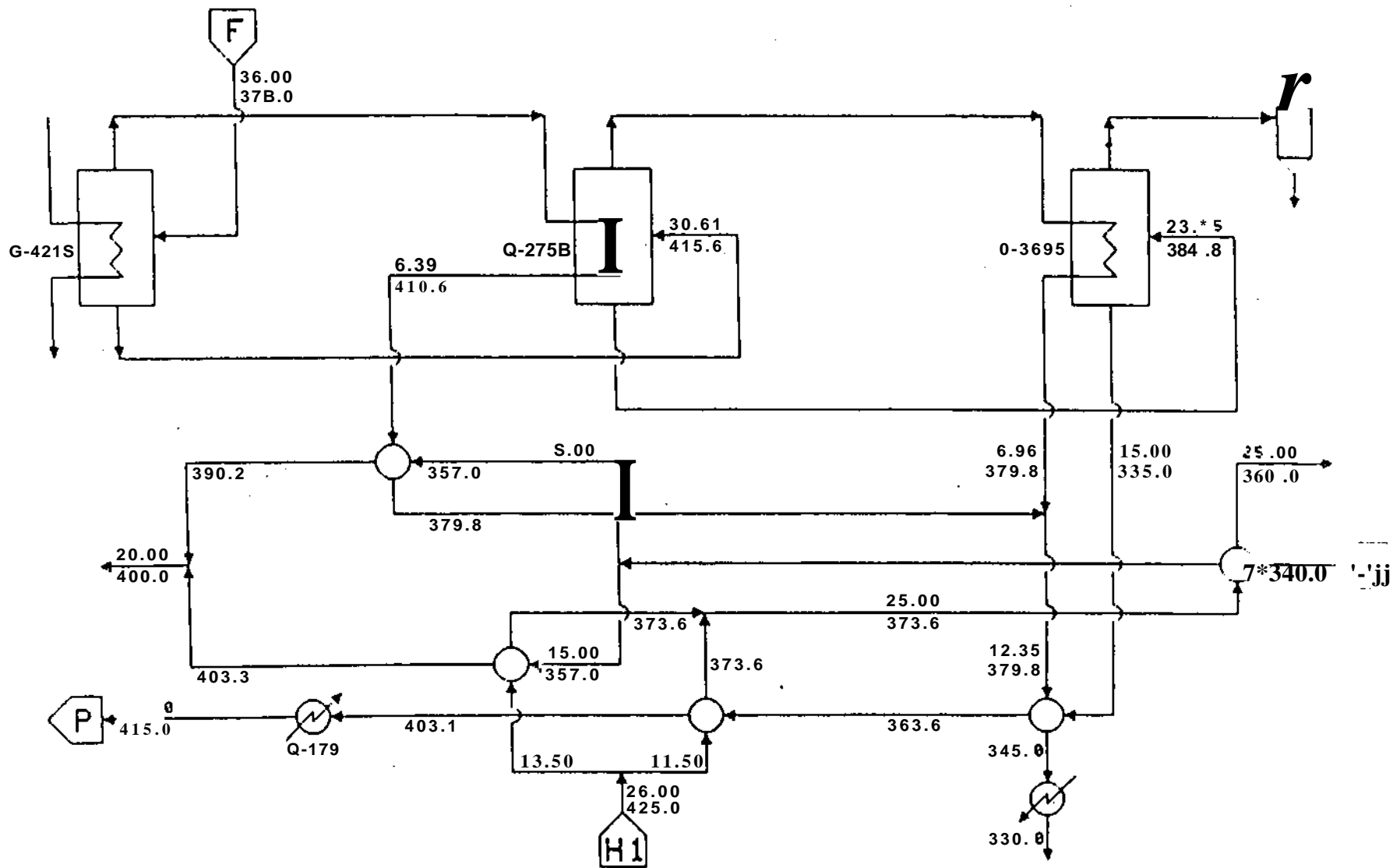


Figure 17: Triple-Effect System with Minimal Heat Integration

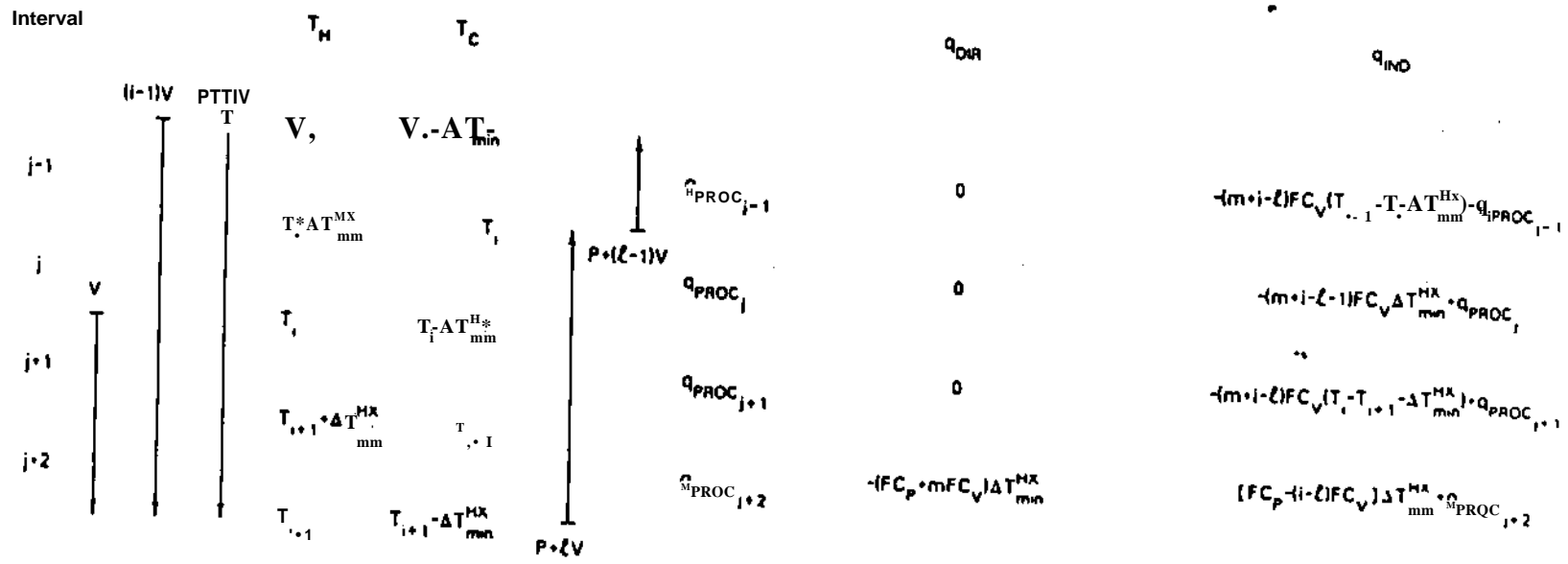


Figure 18: Hot Feed Skipping Effect j

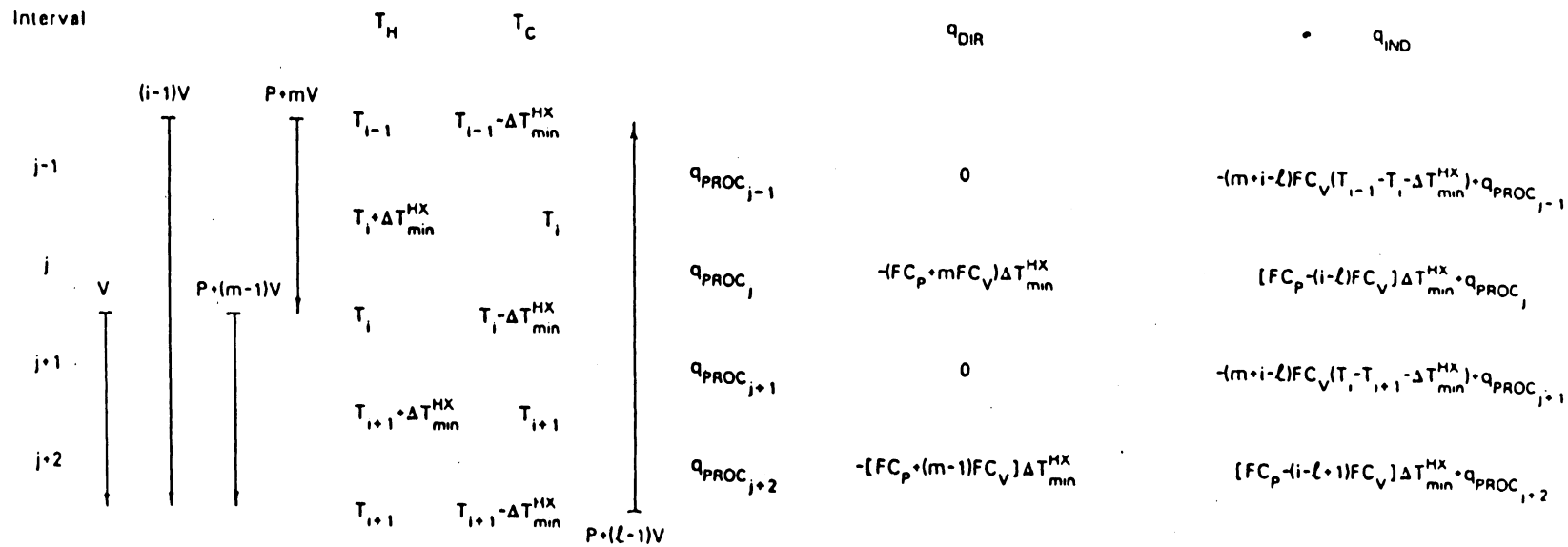


Figure 19: Hot Feed Entering Effect i

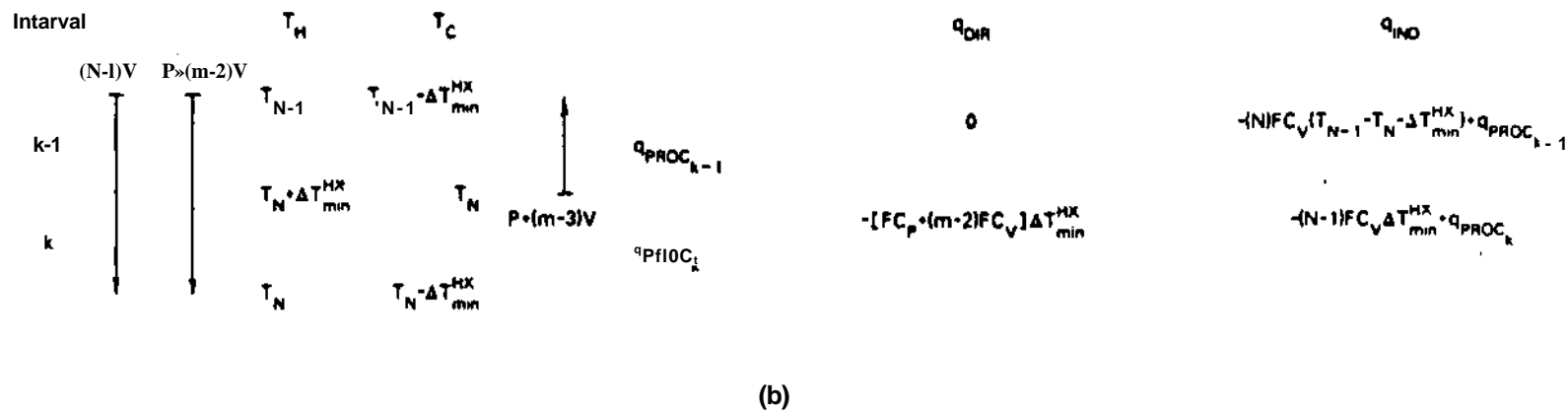
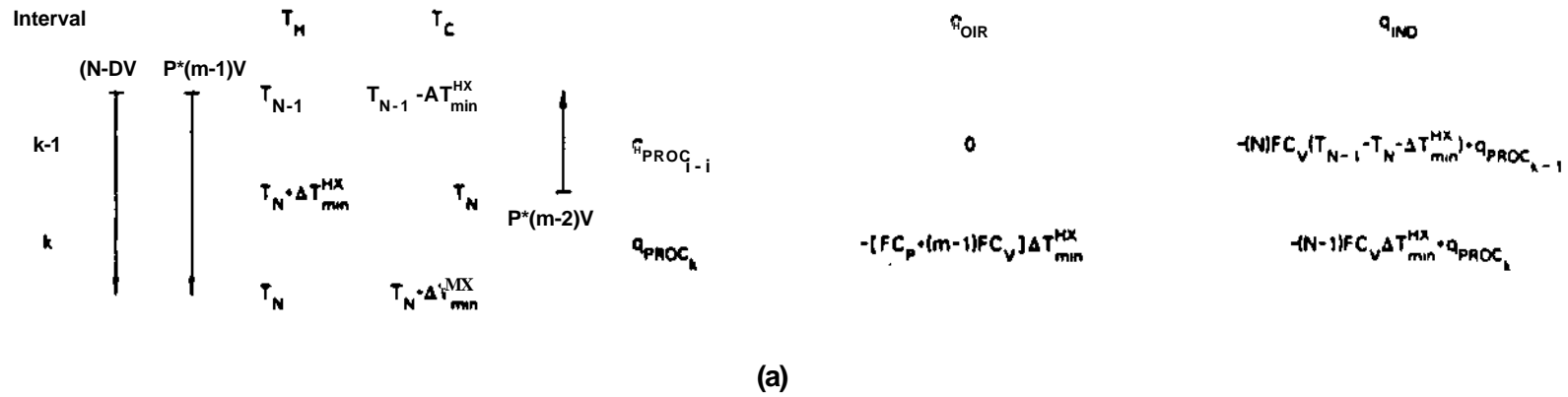


Figure 20: Effect N for Cases (a) and (b)

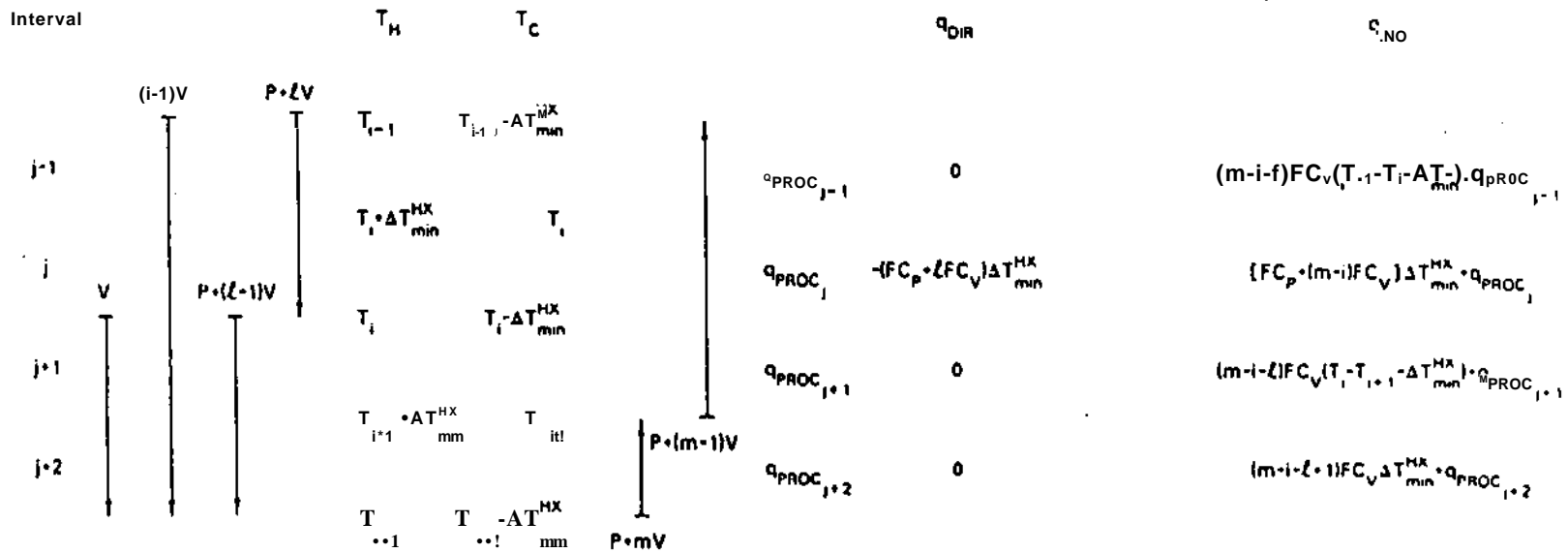


Figure 21: Cold Feed Skipping Effect i

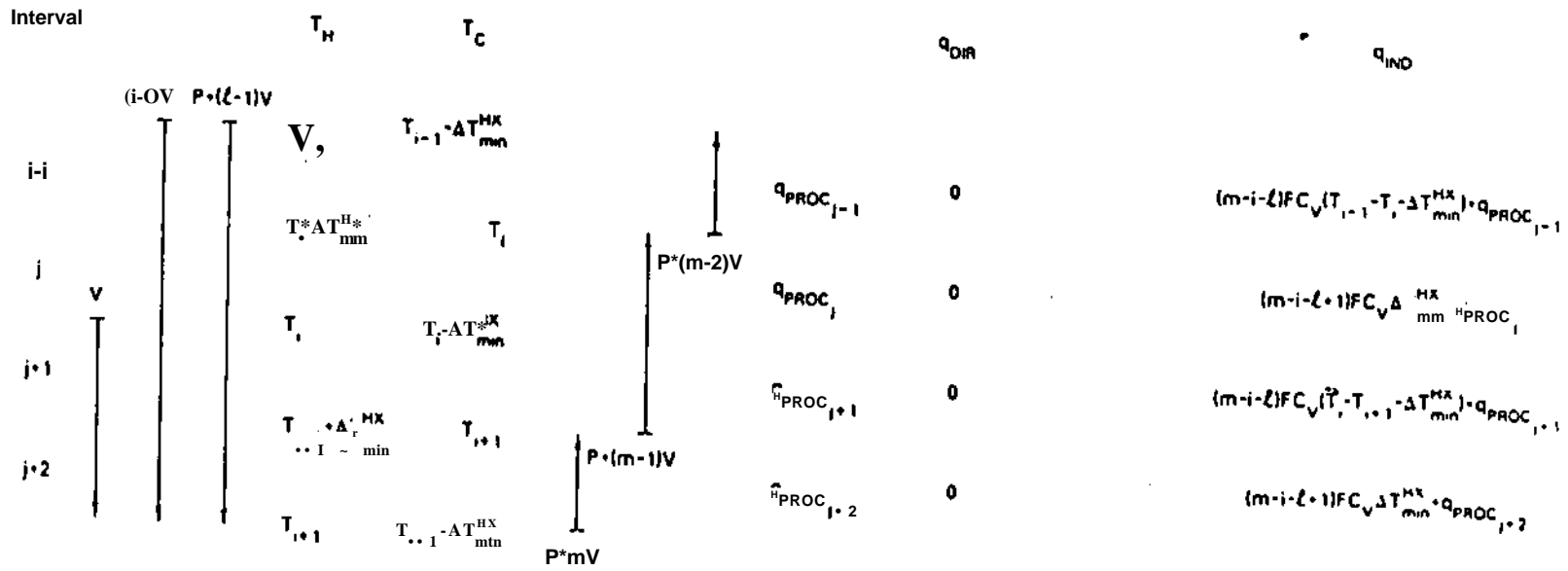
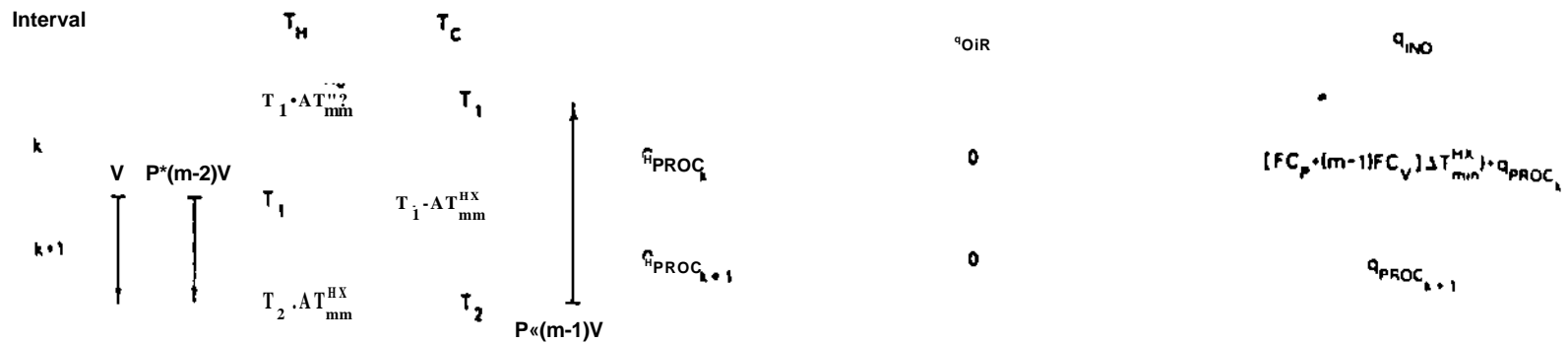
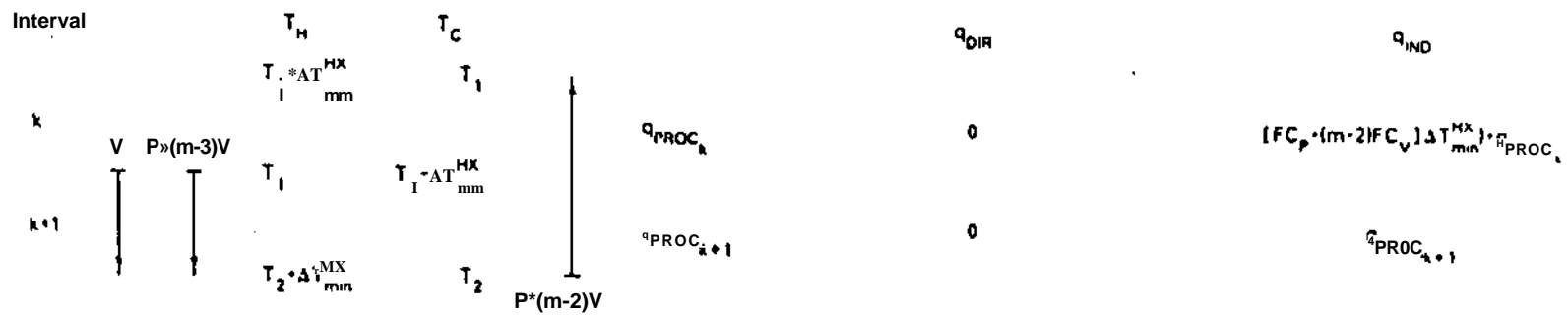


Figure 22: Cold Feed Entering Effect i



(a)



(b)

Figure 23: Effect 1 for Cases (c) and (d)

References

- [1] Cerda, J., A. W. Westerberg, D. Mason, and B. Linnhoff.
Minimum Utility Usage in Heat Exchanger Network Synthesis.
Chemical Engineering Science 38:373-87, March, 1983.
- [2] Guthrie, K. M.
Capital Cost Estimating.
Chemical Engineering 76(6):114-41, March 24, 1969.
- [3] Harper, J. M. and T. F. Tsao.
Evaporator Staging and Optimization (in Computer Programs for Chemical Engineering Education).
In Jelinek, R. (editor), *Computer Programs for Chemical Engineering Education*, pages 117-45. Aztec Publishing, Austin, Texas, 1972. Volume VI Design.
- [4] Hohmann, E. C.
Optimum Networks for Heat Exchange.
PhD thesis, University of Southern California, 1971.
- [5] Holland, C. D.
Fundamentals and Modeling of Separation Processes.
Prentice-Hall, Englewood Cliffs, New Jersey, 1975.
- [6] Itoh, J., K. Shiroko, and T. Umeda.
Extensive Applications of the T-Q Diagram to Heat Integrated System Synthesis.
PSE '82. Japan, August.
- [7] Kern, D. Q.
Process Heat Transfer.
McGraw-Hill, New York, 1950.
375-452.
- [8] King, C. J.
Separation Processes.
McGraw-Hill, New York, 1980.
Second Edition, 155-7, 785-90.
- [9] Linnhoff, B.
Thermodynamic Analysis in the Design of Process Networks.
PhD thesis, University of Leeds, England, 1979.
- [10] Linnhoff, B., D. W. Townsend, D. Boland, G. F. Hewitt, B. E. A. Thomas, A. R. Guy, and R. H. Marsland.
A User Guide on Process Integration for the Efficient Use of Energy.
The Institution of Chemical Engineers, Rugby, Warks, England, 1982.
- [11] McCabe, W. L. and J. C. Smith.
Unit Operations of Chemical Engineering.
McGraw-Hill, New York, 1976.
Third Edition, 427-63.

- [12] Newell. R. B. and D. G. Fisher.
Model Development. Reduction, and Experimental Evaluation for an
Evaporator.
Ind. Eng. Chem. Process Des. Develop. 11(2):213-21. 1972.
- [13] Newell. R. B.
A Comparative Study of Model and Goal Coordination in the Multilevel
Optimization of a Double-Effect Evaporator.
Can. J. of Chem. Eng. 58(2):275-8, April. 1980.
- [14] Nishida. N. G. Stephanopoulos, and A. W. Westerberg.
A Review of Process Synthesis.
AIChE J. 27(3):321-5i. May, 1981.
- [15] Nishitani. H. and E. Kunugita.
The Optimal Flow-Pattern of Multiple Effect Evaporator Systems.
Computers and Chemical Engineering 3(1-4):261-68, 1979.
- [16] Nishitani. H. and E. Kunugita.
Multi-Objective Analysis for Energy and Resource Conservation in an
Evaporation System.
Second World Congress of Chemical Engineering. Canada. 1981.
- [17] Papoulias. S. A. and I. E. Grossmann.
A Structural Optimization Approach in Process Synthesis. Part II: Heat
Recovery Networks,
to appear in *Computers and Chemical Engineering*. London, 1983b.
- [18] Radovic, L. R., A. Z. Tasic. D. K. Grozdanic, B. D. Djordjevic. and V. J.
Valeric.
Computer Design and Analysis of Operation of a Multiple-Effect
Evaporator System in the Sugar Industry.
I & EC Process Design and Development 18(2):318-23, April, 1979.
- [19] Schrage. L. E.
User's Manual for LINDO.
The Scientific Press. Palo Alto, 1981.
- [20] Slota, L.
Improvement of Evaporator Steam Economy by Heat Recovery.
The Chemical Engineer 294:84-90, February, 1975.
- [21] Standiford. F. C.
Evaporation.
Chemical Engineering 70(25);158-76, December 9, 1963.
- [22] Standiford. F. C.
Evaporation.
In Perry, R. H. and C. H. Chilton (editors). *Chemical Engineers' Handbook*.
pages 11(27-38). McGraw-Hill. New York. New York, 1973.
Fifth Edition.

- [23] **Stewart, G. and G. S. G.** Beveridge.
Steady-State Cascade Simulation in Multiple Effect Evaporation.
Computers and Chemical Engineering 1(1):3-9. 1977.